REPORT

REDWIN

DAMPING RATIO FROM LABORATORY TESTS

DOC.NO. 20150014-01-R
REV.NO. 0 / 2016-06-02

NORWEGIAN GEOTECHNICAL INSTITUTE
NGI.NO

Project

Project title:	REDWIN
Document title:	Damping ratio from laboratory tests
Document no.:	20150014-01-R
Date:	2016-06-02
Revision no. /rev. date:	0

Client

Client:	Research Council of Norway
Client contact person:	Harald Rikheim
Contract reference:	243984/E20

for NGI

Project manager:	Amir Kaynia
Prepared by:	Knut H. Andersen
Reviewed by:	Finn Løvholt

Summary

This report presents the material soil damping ratio determined from cyclic DSS and triaxial and resonant column laboratory tests on normally consolidated clay and cyclic DSS and triaxial laboratory tests on dense sand. The damping ratios presented are derived by using an improved method for interpretation of the damping, taking into account the influence of permanent strain accumulation. The report seeks to present an overview of the damping behaviour as a function of strain and number of load cycles for various soils and test conditions. It also compares the damping ratio measured in the laboratory tests to damping ratio from Seed and Idriss (1970) and Darendeli (2001).

The tests on clay were run on high, medium and low plasticity clays as well as on a quick clay. The tests on sand were run on two batches of fine to medium Dogger Bank sand (Blaker and Andersen, 2015). Batch A had essentially no fines, and Batch B had about 20% fines. Triaxial and DSS tests were run on two relative densities, D_r=100% and 80%, in a normally consolidated state. The D_r=80% specimens were also tested at an overconsolidation ratio of 4.

NORWEGIAN GEOTECHNICAL INSTITUTE
NGI.NO

Main office
PO Box 3930 Ullevaal St.
NO-0806 Oslo
Norway

Trondheim office
PO Box 5687 Sluppen
NO-7485 Trondheim
Norway

T 22 02 30 00
F 22 23 04 48
NGI@ngi.no

BIC NO. DNBANOKK
IBAN NO26 5096 05 01281
COMPANY NO.
958 254 318MVA

ISO 9001/14001
CERTIFIED BY BSI
FS 32989/EMS 612006

The shape of the stress strain curves during cyclic loading is different for normally consolidated clay and dense sand. The damping ratio increases with cyclic shear strain during the first cycles of a DSS test on dense sand, but reaches a maximum value and starts to decrease with increasing shear strains and number of cycles. Normally consolidated clays do not show a reduction in damping ratio with increasing N to the same extent as the dense sand. It is believed that the reason for the difference is that a normally consolidated clay contracts, whereas a dense sand dilates when the shear strain increases. It is therefore expected that loose sands will show the same tendency as the normally consolidated clays, and that overconsolidated clays will show the tendency observed in dense sand.

The consequence of the observed behaviour is that the damping ratio is not a function of cyclic shear strain only, but may decrease with increasing number of cycles for a given cyclic shear strain. The effect of number of cycles is most pronounced in dilating soil, like dense sand, and less for contracting soil, like normally consolidated clay.

The increase in damping ratio during the first cycles in the DSS tests is less pronounced or does not exist in the triaxial tests, except in overconsolidated sand. The reason for the difference during the first cycles may be that the shear stress in the triaxial tests on normally consolidated sand cycles around an average shear stress, whereas the shear stress cycles around zero average shear stress in the DSS tests and the triaxial tests on overconsolidated sand.

The results from tests on normally consolidated clay further show that the damping ratio:

- increases with increasing cyclic shear strain.
- depends on the number of cycles for the low plasticity clay. The effect is less pronounced for quick clay and high plasticity clay.
- is higher in the low plasticity clay than in the high plasticity clay and the quick clay
- increases with increasing average shear stress. The lowest damping ratio seems to occur for DSS tests with symmetrical cyclic loading.
- tends to increase with increasing load period
- is very similar in remoulded and intact samples of high plasticity clay.

The results from tests on dense sand show that the damping ratio:

- increases with increasing cyclic shear strain and decreases with increasing number of cycles.
- is somewhat higher for Dr=80% than for Dr=100% for low N. The damping ratio in DSS tests on sand with Dr=80% and N=10 is significantly lower than the N=10 curve for Dr=100%.
- does not seem to be influenced by fines content in the triaxial tests, but has some tendency to decrease with increasing fines content in DSS tests on sand with Dr=100%.

The effect of other parameters on the damping ratio in dense sand was studied by running tests where these parameters were varied. The effects are relatively modest, and since the number of tests with different parameters was limited, some of the observed differences may be due to scatter in the data. There is, however, some tendency for the damping ratio to:

- be lower in overconsolidated than in normally consolidated sand at low N (N=1 to 10)
- increase with decreasing consolidation stress in triaxial tests on overconsolidated sand with D_r=80% and in DSS tests.
- increase with precycling for N=10 to 30 in DSS tests on sand with D_r=80% and in triaxial tests
- be lower for τ_a>0 than for τ_a=0 at small N, and higher for τ_a>0 than for τ_a=0 when N>10 for DSS tests with D_r=80%. The damping ratio tends to be lower for undrained than for drained τ_a.

The damping ratio is less influenced by τ_a for DSS tests with D_r=100% and low N. There is some tendency for the damping ratio to be smaller for tests with τ_a>0 than for tests with τ_a=0 at N=10 and higher. In the triaxial tests, there is no clear effect of average shear stress, neither for drained nor undrained change in average shear stress.

Seed and Idriss (1970) and Darendeli (2001) give no guidance for non-symmetrical cyclic loading or for triaxial type loading. The range between the upper and lower Seed and Idriss (1970) damping ratio curves is quite significant. Comparisons with damping ratio curves from Seed and Idriss (1970) show that the damping ratio in simple shear tests with symmetrical cyclic loading:

- generally falls within the upper and lower Seed-Idriss (1970) curves for clay.
- is between the lower and the mean Seed-Idriss (1970) curves for sand with D_r=100% and N=1 to about 10 , but can be significantly lower for higher N.
- is significantly lower than the lower Seed-Idriss (1970) curve for sand with D_r=80% and N=10.
- is significantly more influenced by N than indicated by the formula for sand in Seed and Idriss (1970).

Comparisons of the damping ratio curves from Darendeli (2001) and the damping ratio in simple shear tests with symmetrical cyclic loading show that:

- For clay:
  - The Darendeli (2001) curves generally give lower damping ratio than the test data at small (<0.3%) and high (>3%) cyclic shear strains. At intermediate strains, the Darendeli (2001) curves give similar, lower, and higher damping ratio than measured for high plasticity, low plasticity and quick clays, respectively.
  - The effect of load period in the Darendeli (2001) expression at low γ_{cy} can be questioned, as it gives a negative damping ratio for a 100s load period. It seems that the effect of load period may be underestimated at higher γ_{cy}.

- The Darendeli (2001) curves show smaller effect of number of cycles than what the test results for quick clay and, to some extent, the high plasticity clay seem to indicate.

For sand, the Darendeli (2001) curves

- do not reflect the large effect of N seen in the tests on dense sand.
- overestimate the damping ratio for high N. This is important to note for fatigue analyses where the number of representative cycles can be high.
- generally give damping ratio close to measured in the intermediate strain range (γ_{cy}=0.1% - 1%) for clean sand for N<5, but overestimate the damping ratio for N>5. The same is true for the sand with 20% fines, but for N=1 instead of N=5.
- give reasonable agreement with the tests in the high strain range (γ_{cy}>1%) for N=25 in the clean sand with D_r=100% and for N=5 for clean sand with Dr=80% and for the sand with 20% fines. The damping ratio is underestimated for lower N and overestimated for higher N.
- predict similar effect of σ_{vc}' as seen in the tests.
- predict no effect of overconsolidation ratio, which agrees with only a small tendency for the damping ratio to decrease with increasing overconsolidation ratio in the tests.

Contents

Review and reference page

1 Introduction

This report presents the damping ratio determined from cyclic DSS and triaxial laboratory tests on clay and sand. The laboratory tests have been performed as part of other projects, but the interpretation of the damping ratio has previously not been done.

Damping ratio data has been published previously, by for instance Seed and Idriss (1970) and Darendeli (2001), and the damping ratio determined in this project is compared to the data in these references.

The work is a deliverable to the REDWIN project, which brings together experts from geotechnical and structural engineering, in order to jointly develop better methods for reducing costs related to foundation effects on offshore wind turbines. The aim in the REDWIN project is to establish new models describing soils and foundations that will be integrated with the computational tools used by structural engineers today. This will contribute to optimized engineering and design, resulting in less expensive offshore wind energy. REDWIN is co-funded by the Research Council of Norway (80%) as well as by Statoil (10%) and Statkraft (10%).

2 Definition of damping ratio, D

The material soil damping ratio *D* is here defined as the ratio between the energy loss over a cycle, ΔW, and the potential energy, W:

$$D = \frac{\eta}{2} = \frac{1}{4\pi}\frac{\Delta W}{W}$$

where the hysteretic loss factor is denoted η. The shaded area enclosed within the loop in a cycle, depicted as an elliptically shaped loop in Figure 2.1, represents the energy lost per unit soil volume in that load cycle, caused by the material behaviour of the soil. This energy loss can be expressed as:

$$\Delta W = \oint \tau(\gamma) \cdot d\gamma$$

Similarly, the potential energy corresponds to the shaded triangle in Figure 2.1, defined by the product of the maximum cyclic stress and maximum cyclic strain. The methodology used to derive the damping values in this report is adopted from NGI (2014) to take into account the permanent accumulation of strain. In the procedure, attempts are made to close the stress strain loops by subtracting the permanent accumulation within each loop assuming a linear stress strain variation within a single loop.

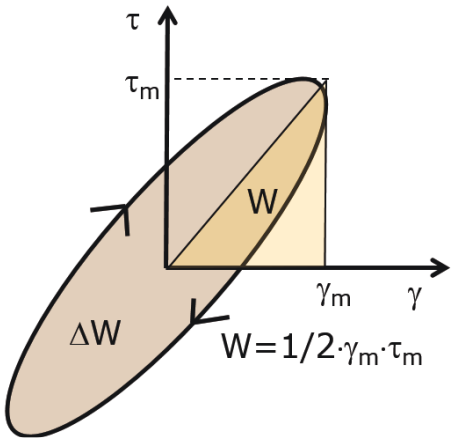

Figure 2.1 Principle sketch of a simplified stress-strain loop during pure cyclic loading. The stress and strain are denoted by τ and γ respectively. Maximum stress and strain values are denoted by the "m" subscripts.

The shape of the stress-strain curve of a soil will depend on whether the soil tends to contract or dilate when it is sheared. Typical stress-strain curves for DSS tests on normally consolidated clay are presented in Figure 2.2 for a test with symmetrical cyclic loading (average shear stress τ_a=0), and in Figure 2.3 for a test with non-symmetrical cyclic loading (τ_a>0). Triaxial tests consolidated to an anisotropic stress condition (τ_c>0) will behave like the test in Figure 2.3.

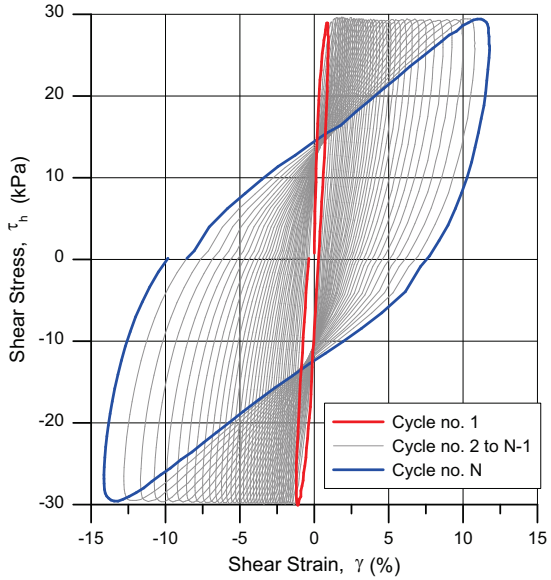

Figure 2.2 Stress strain curves from cyclic DSS test on high plasticity clay with symmetrical cyclic loading

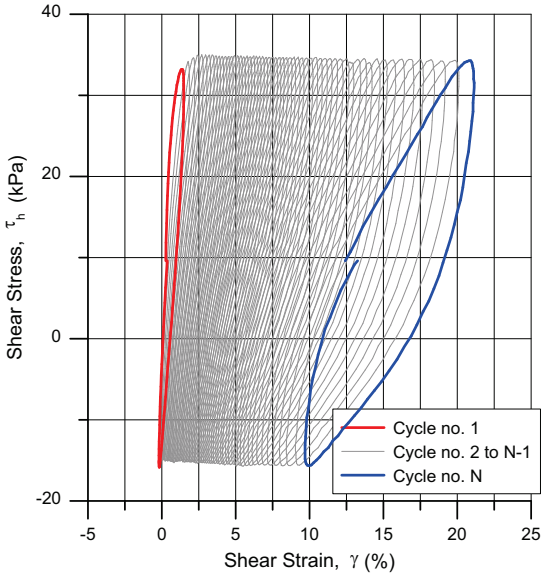

Figure 2.3 Stress strain curves from cyclic DSS test on high plasticity clay with non-symmetrical cyclic loading

Typical stress-strain curves for tests on dense sand are presented in Figure 2.4 for a test with symmetrical cyclic loading (τ_a=0), and in Figure 2.5 for a test with non-symmetrical cyclic loading (τ_a>0).

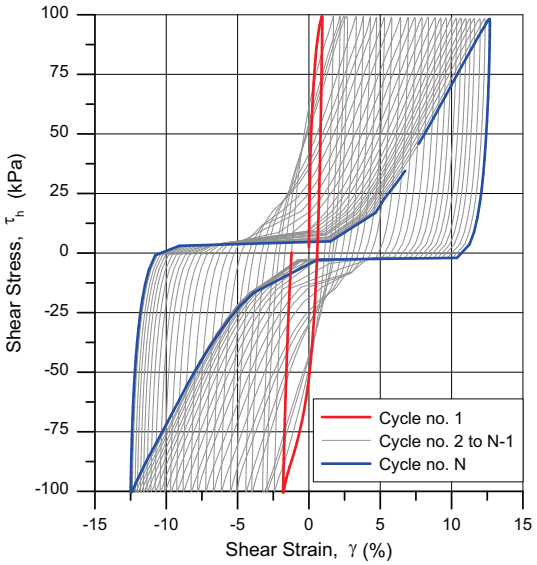

Figure 2.4 Stress strain curves from cyclic DSS test on dense sand with symmetrical cyclic loading

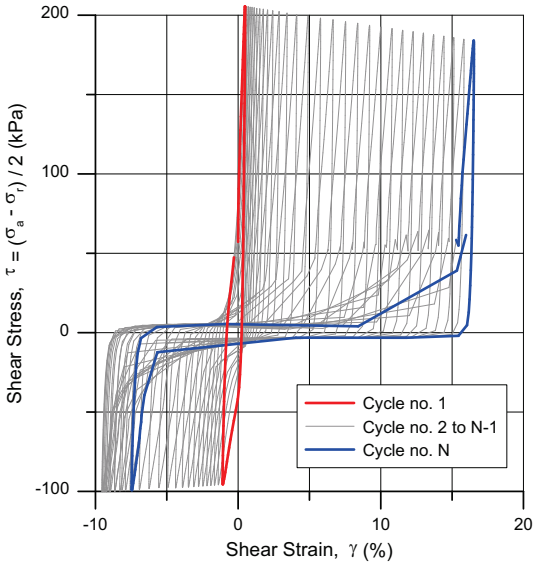

Figure 2.5 Stress strain curves from cyclic triaxial test on dense sand with non-symmetrical cyclic loading

The shape of the stress strain curves of normally consolidated clays and dense sand are initially more or less elliptical. The normally consolidated clays retain this shape to large shear strains, whereas the shape changes significantly for dense sand. Both soils experience generation of excess pore pressure due to cyclic loading, but the reason for the difference is that the normally consolidated clay contracts and the dense sand dilates when the shear strain increases. It is expected that loose sands that contract during shearing will show the same tendency as normally consolidated clay, and that overconsolidated clays will show the tendency observed in dense sand.

One should notice how the damping ratio is calculated for a dilating soil with non-symmetrical cyclic loading. This is illustrated in Figure 2.7, which shows that the contribution to the damping is not symmetrical around the average shear stress.

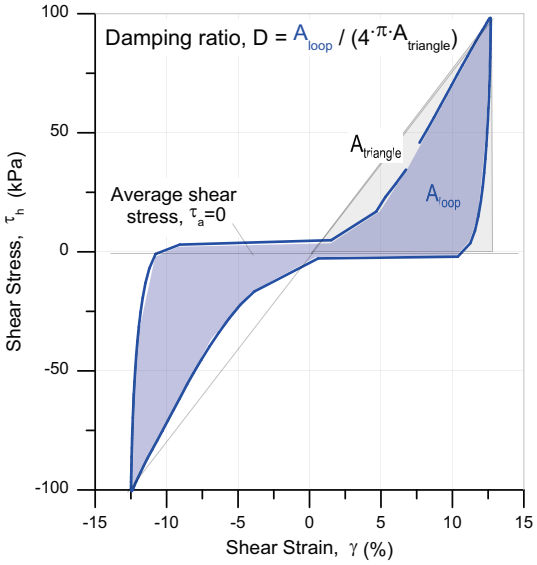

Figure 2.6 Calculation of damping ratio in dense sand with symmetrical cyclic loading

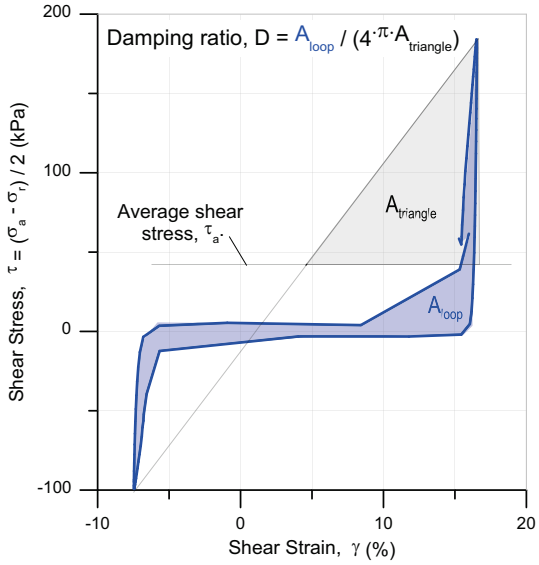

Figure 2.7 Calculation of damping ratio in dense sand with non-symmetrical cyclic loading

3 Soil types

Damping ratios of normally consolidated clays and dense sands are presented in this report. The soil characteristics and the test types are specified in Table 3.1 for the clays and in Table 3.2 for the sands.

3.1 Clays

Four close to normally consolidated clays are investigated (Table 3.1). The clay fraction ranges between 22% and 75%. The plasticity index, I_p, ranges between 8% and 84%. The low I_p (8% to 11%) is for a quick clay, which has a clay fraction of about 37%. Since the clay fraction is so high, the low I_p may not be representative for a non-sensitive, lean clay.

DSS tests were performed on three of these clays, resonant column tests on two of the clay types, and triaxial tests on 1 of the clay types. Tests with 10s load period were run on all the clays. In addition, a load period of 100s was included for the high plasticity clay and 1s for the quick clay. Tests were run on intact samples for all of the clays, and in addition on remoulded samples of the high plasticity clay.

Table 3.1 Clay characteristics and test types. I_p denotes plasticity index, S_t the soil sensitivity, w the water content, and OCR the overconsolidation ratio

Name	I_p (%)	S_t	% clay	w (%)	OCR	Test types	Parameters
High plasticity clay	75-84	2.3	65-75	77-86	1.35	Triaxial & DSS	Intact & remolded T=10 & 100s
Medium plasticity clay	37	5.5	45	~50	1.45	Res. col.	Intact
Low plasticity clay	17-20	2-3	22-37	15-23	1.45	DSS Res. col.	Intact T=10s
Quick clay	8-11	75-100	36-38	35	1.5	DSS	Intact T=1 & 10s

3.2 Sands

The sand tests were run on fine to medium Dogger Bank sand (Blaker and Andersen, 2015). Two different batches were used. Batch A had essentially no fines, and Batch B had about 20% fines.

The specimens were prepared by moist undercompaction. Relative density of about 80% and 100% was studied. The specimens were subjected to drained pre-shearing before the main undrained cyclic loading. The preshearing level, the consolidation stress and the overconsolidation ratio were varied to quantify the effect of these parameters on the damping ratio. Details are given in Table 3.2. All the tests on sand were run with 10s load period. The triaxial tests were consolidated to a horizontal effective stress of $\sigma_{hc}'=K_0 \cdot \sigma_{vc}'$, where $K_0=0.45$ for normally consolidated sand and $K_0=1.0$ for overconsolidated sand.

Table 3.2 Sand characteristics and test types. D_r denotes the relative density, and σ_{vc}' the effective vertical stress

Name	<0.002 %	<0.06 %	D_{10} mm	Test types	D_r %	w_{after} %	OCR	σ_{vc}' kPa	Preshearing N=400
Dogger Bank A	0	<1	0.017	Triaxial & DSS Drained & undrained $\Delta\tau_a$	~100	~22.3	1	200	$\tau_{cy}=0.06\sigma_{vc}'$ $\tau_{cy}=0.12\sigma_{vc}'$
								40	$\tau_{cy}=0.06\sigma_{vc}'$
					~78	~24.4	1	200	$\tau_{cy}=0.06\sigma_{vc}'$ $\tau_{cy}=0.12\sigma_{vc}'$
								40	$\tau_{cy}=0.06\sigma_{vc}'$
					~80	~24.3	4	200	$\tau_{cy}=0.06\sigma_{vc}'$ $\tau_{cy}=0.12\sigma_{vc}'$
								40	$\tau_{cy}=0.06\sigma_{vc}'$
Dogger Bank B	<1	20	0.087		~100	~17.7	1	200	$\tau_{cy}=0.06\sigma_{vc}'$
					~80	~20	1	200	$\tau_{cy}=0.06\sigma_{vc}'$

4 Damping ratio for clays

4.1 Damping ratio in DSS tests for different clay types

The damping ratio in DSS tests with symmetrical cyclic loading (τ_a=0) is plotted as a function of cyclic shear strain in Figure 4.1 for the three different clays investigated. All the results presented are for tests with a 10s load period. The damping ratio from resonant column data on low and medium plasticity clays are also included. The damping ratio curves from Seed and Idriss (1970) for clay are included as background in all the figures.

The results show that:

- The damping ratio increases with increasing cyclic shear strain
- The high plasticity clay and the quick clay are similar, apart from one test on the high plasticity clay (PC-G42-s12-G1) which gives lower D than the other. The low plasticity clay gives higher D at a given γ_{cy}. This effect of plasticity is found in both the DSS and the resonant column tests.

More specifically:

- For the high plasticity clay, D may be defined by one curve with D increasing with γ_{cy}, even if the data for N=1 tend to plot a little higher than the data for N>1.
- For the quick clay, the tendency for drop in D at low N is more pronounced than for the high plasticity clay, and curves with D as function of γ_{cy} will thus be a function of N. D has a tendency to decrease during the first ~10 cycles, but D increases again with γ_{cy} after about 10 to 100 cycles. The lowest D generally occurs at about N=5 to 10 cycles. D vs. γ_{cy} seems relatively independent of N after about 10 to 100 cycles.
- For the low plasticity clay, the different tests do not define one common curve, and D seems to depend on both γ_{cy} and N. It must be noted, however, that D has been determined by an old version of the interpretation software for 7 of the 10 tests on the low plasticity clay. The data files for these 7 tests have not been available.
- The damping ratio of the 3 three clay types generally falls within the upper and lower curves from Seed-Idriss (1970), but the D for the high plasticity clay and the quick clay are below the mean Seed-Idriss (1970) curve, and even below the lower Seed-Idriss curve at large cyclic shear strains (γ_{cy} >2%).
- Some noise is evident for some of the tests and particularly when the strain is low. The damping interpretation method is sensitive to low resolution sampling which produces such spurious noise.

4.1.1 Effect of average shear stress on damping ratio in DSS tests on clay

The damping ratio in DSS tests with non-symmetrical cyclic loading ($\tau_a>0$) is compared with the damping ratio for tests with symmetrical cyclic loading for the high plasticity clay in Figure 4.2 and for the quick clay in Figures 4.3a and b.

The average shear stress, τ_a, is applied undrained in the tests on high plasticity clay. The damping ratio increases with increasing τ_a for a given γ_{cy}, but seems reasonably independent of N. The behavior of the test with $\tau_a=0.49s_u$ deviates from the others in that D increases with γ_{cy} during the first few cycles, but then decreases with increasing N and γ_{cy}. This behavior is also seen in the duplicate test on remolded clay and may hence be consistent (Figure 4.4).

The average shear stress, τ_a, is applied drained in the tests on quick clay. Figure 4.3a and b show results for load period of 10s and 1s, respectively. There is significant noise in the data for $\gamma_{cy} \leq 0.1\%$, but the damping ratio increases with increasing τ_a for a given γ_{cy}. The damping ratio seems to decrease with increasing γ_{cy} during the first ~10 cycles, and then to increase with increasing γ_{cy} after about 10 to 100 cycles. The damping ratio γ_{cy} is thus a function of both γ_{cy}, τ_a and N.

4.1.2 Effect of remoulding on damping ratio in DSS tests on high plasticity clay

Tests with $\tau_a=0$ and $\tau_a=0.47 \cdot s_u$ were run on remoulded high plasticity clay. The results are presented in Figure 4.4. The curves for tests on remoulded clay are dotted. Comparison with tests on intact clay shows that the damping ratio of remoulded and intact high plasticity clays is very similar.

4.1.3 Effect of load period on damping ratio in DSS tests on clay

Most of the tests are run with 10s load period. However, two DSS tests with T=100s were run with $\tau_a=0$ and $\tau_a=0.3s_u$ on the high plasticity clay, moreover, 16 tests with T=1s were run with various τ_a on the quick clay.

The results from tests with T=100s and 10s on the high plasticity clay are compared in Figure 4.5. The curves for tests with T=100s are dotted. The comparison shows that there is a tendency for D to increase with increasing load period.

The results from tests with T=1s and 10s on the quick clay are compared in Figure 4.6. Only results from tests where similar τ_a-values are available for the two load periods are included. There may be some tendency for the damping ratio to decrease with decreasing load period, but the tendency is less clear than for the high plasticity clay.

4.2 Damping ratio in triaxial tests on high plasticity clay

The damping ratio in cyclic triaxial tests with different average shear stress, τ_a, on high plasticity clay is shown in Figure 4.7. The samples were consolidated with a K_0'=0.55, corresponding to $\tau_a=\tau_0=0.45s_u$. The change in average shear stress $\Delta\tau_a=\tau_a-\tau_0$ was applied under undrained conditions.

The results show that D vs. γ_{cy} is relatively independent of N for $\tau_a=\tau_0=0.45s_u$. For other values of τ_a, however, D is a function of both τ_a and N. D drops markedly from N=1 to 2, and continues to drop during the next ~3 to 10 cycles before it becomes constant or starts to increase. One exception is one of the tests with $\tau_a=\tau_0=0.45s_u$, which does not start to increase with N.

D is close to the lower Seed-Idriss (1970) curve for high N, but generally higher than the lower Seed-Idriss (1970) curve for low N.

4.2.1 Effect of load period on damping ratio in triaxial tests on high plasticity clay

The results from four triaxial tests with T=100s load period are compared to the results from four triaxial tests with 10s load period in Figure 4.8. The curves for tests with T=100s are dotted. The tests are run on the high plasticity clay and with different average shear stresses, as explained in Section 4.3. The comparison shows that there is a tendency for D to increase with increasing load period, as for the DSS tests (Section 4.3).

4.3 Comparison of damping ratio in DSS and triaxial tests on high plasticity clay

The damping ratio measured in DSS and triaxial tests on high plasticity clay is compared in Figures 4.9, 4.10 and 4.11.

The results show that

- DSS with τ_a=0 tend to give the lowest D for given values of γ_{cy} and N.
- triaxial tests give higher D than DSS tests in tests consolidated to the in situ stress conditions ($\tau_a=\tau_0=0.45s_u$ in triaxial tests and τ_a=0 in DSS tests) (Figure 4.10).
- the results from tests with T=100s (Figure 4.11) confirm the results measured in tests with 10s (Figures 4.9 and 4.11).

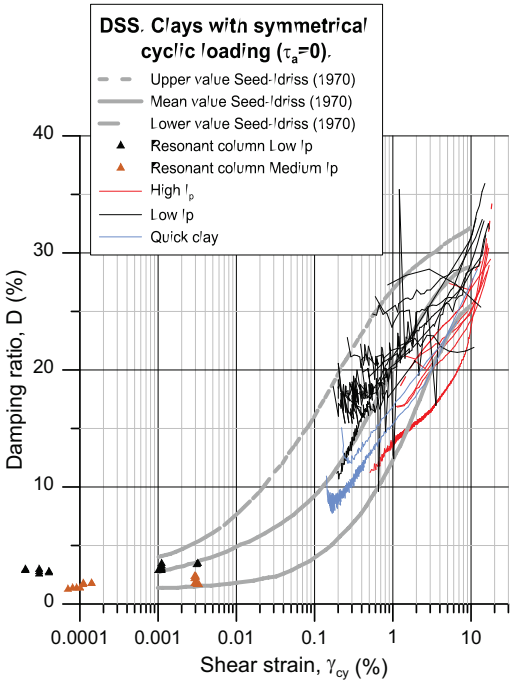

Figure 4.1 Damping ratio as function of cyclic shear strain in DSS tests on 3 different clays. Symmetrical cyclic loading.

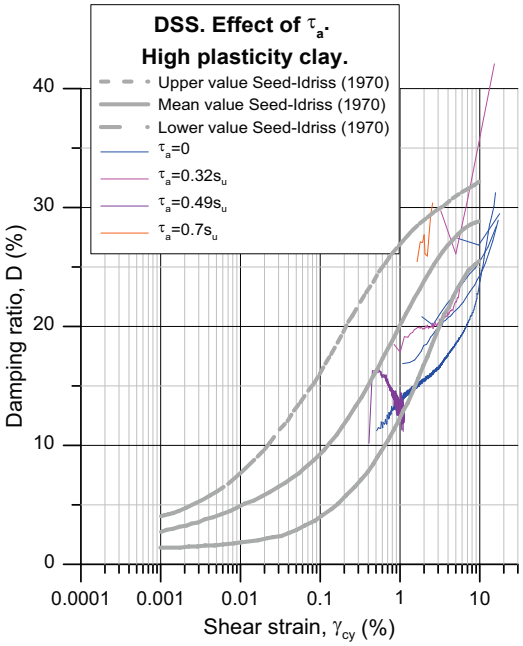

Figure 4.2 Effect of average shear stress on damping ratio in DSS tests on high plasticity clay.

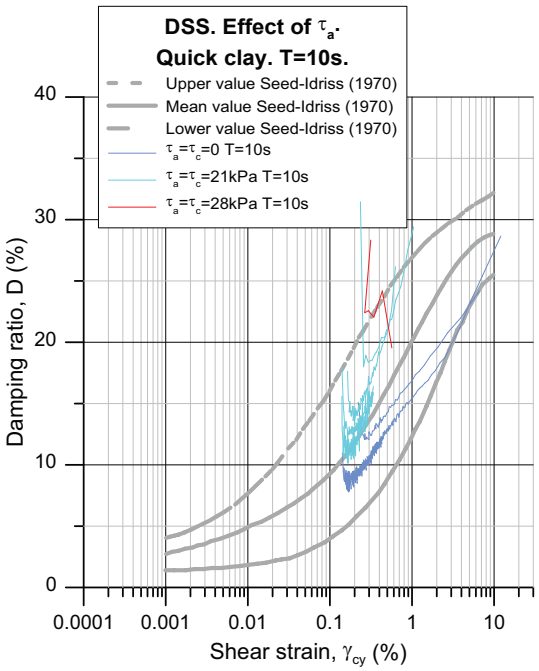

Figure 4.3a Effect of average shear stress on damping ratio in DSS tests on quick clay. T=10s

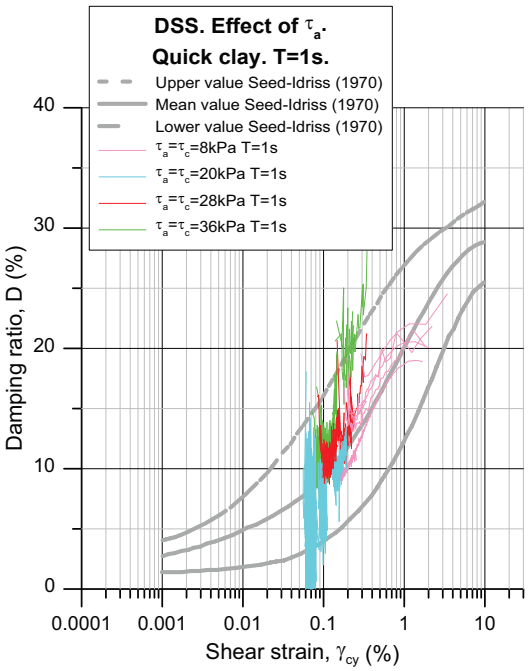

Figure 4.3b Effect of average shear stress on damping ratio in DSS tests on quick clay. T=1s

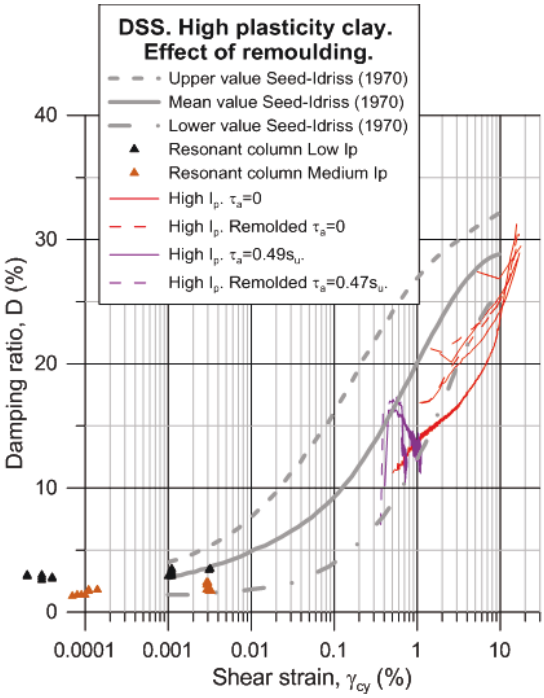

Figure 4.4 Effect of remoulding on damping ratio in DSS tests on high plasticity clay

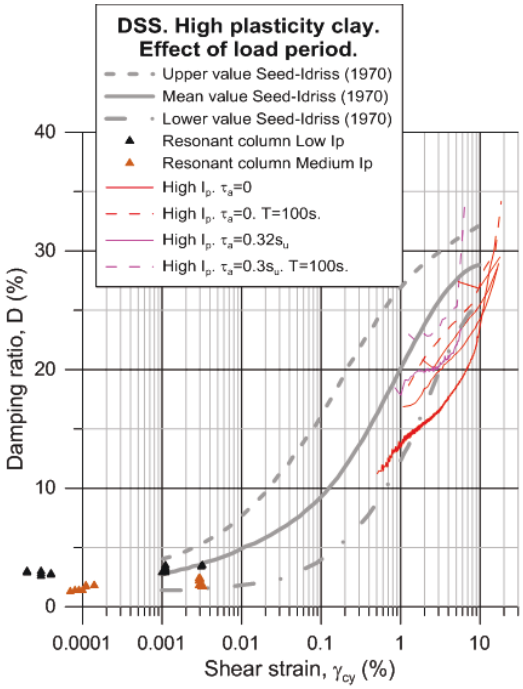

Figure 4.5 Effect of load period on damping ratio in DSS tests on high plasticity clay

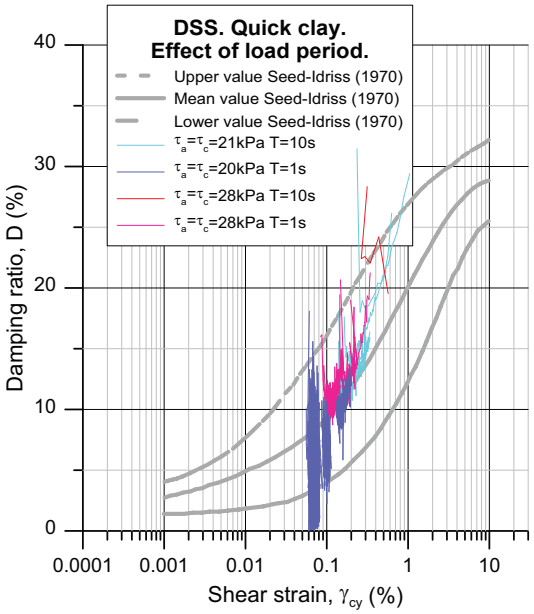

Figure 4.6 Effect of load period on damping ratio in DSS tests on quick clay

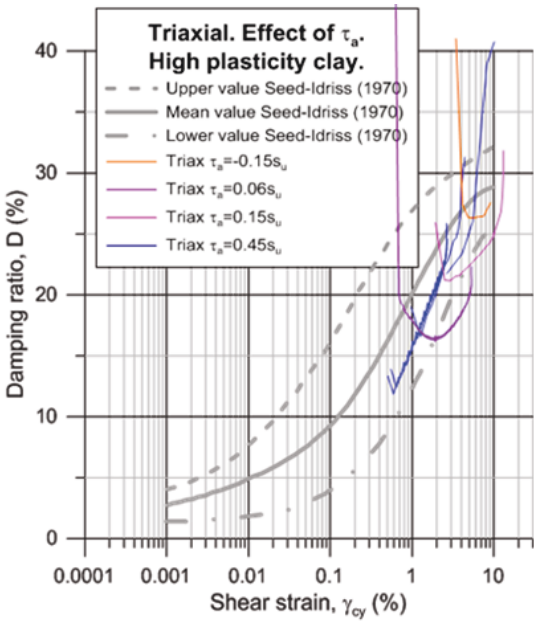

Figure 4.7 Effect of average shear stress on damping ratio in triaxial tests on high plasticity clay

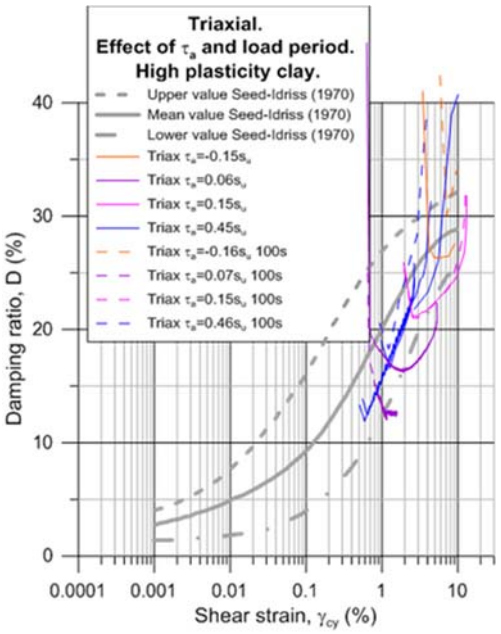

Figure 4.8 Effect of load period on damping ratio in triaxial tests on high plasticity clay

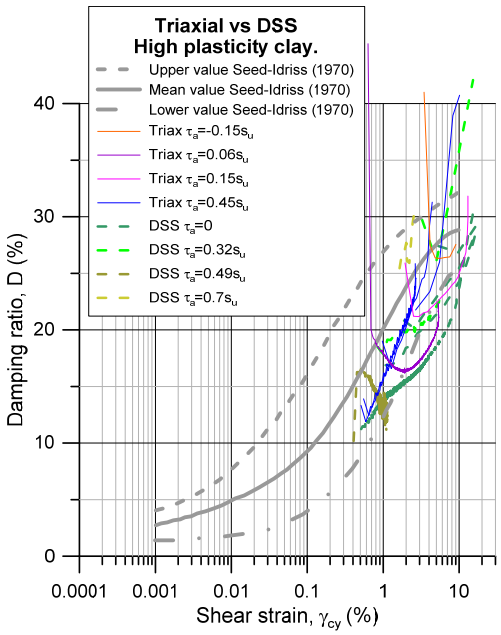

Figure 4.9 Comparison of damping ratio in DSS and triaxial tests on high plasticity clay

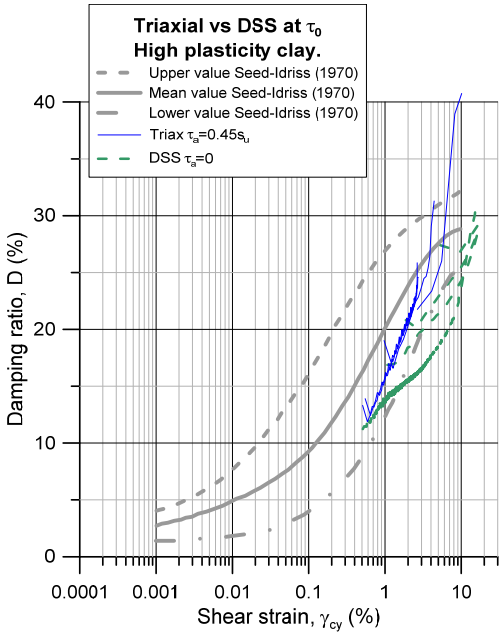

Figure 4.10 Comparison of damping ratio in DSS (τ_a =0) and triaxial tests ($\tau_a = \tau_0 = 0.45s_u$) on high plasticity clay

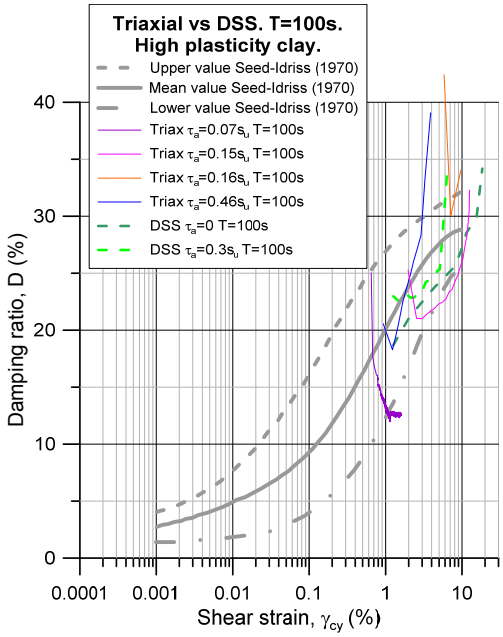

Figure 4.11 Comparison of damping ratio in DSS and triaxial tests with T=100s on high plasticity clay

5 Damping ratio for sands

5.1 Damping ratio in DSS tests on sand

The damping ratio in DSS tests on dense sand depends on both cyclic shear strain and number of cycles, as can be seen from the results of DSS tests with τ_a=0 in Figures 5.1 and 5.2. The damping ratio increases with cyclic shear strain during the first cycles, but reaches a maximum value and starts to decrease with increasing shear strains. One may connect points with the same N to establish curves of damping ratio as functions of cyclic shear strain for given values of N. These curves will plot highest for N=1 and lower the higher N is. The reason for the decrease in damping with N is due to the shape of the stress-strain curve, which changes with number of cycles, as indicated in Figure 2.4. The change in the shape is due to generation of average pore pressure and dilatancy in dense sand.

The normally consolidated clays presented in Section 4 did not show reduction in damping ratio with increasing N to the same extent as for sand. The reason is believed to be that the clays contracted whereas the sand dilated, leading to differently shaped stress-strain curves (Figures 2.2 and 2.4). Most likely the difference in D vs γ_{cy} between the dense sands and the normally consolidated clays observed in the tests in this study is due to the difference in tendency to dilate, and it is therefore expected that loose sand could show similar tendency as the normally consolidated clays, and that overconsolidated clays could show similar tendency as observed in dense sand.

5.1.1 Effect of density on damping ratio in DSS tests on sand

The damping ratio for clean sand with relative density of D_r=100% and D_r=80%, is presented in Figures 5.1 and 5.2, respectively, and compared in Figure 5.3. The damping ratio curves from Seed and Idriss (1970) for sand are included as background in all the figures.

The damping ratio for D_r=100% is close to the lower Seed-Idriss (1970) curve for N=1 to about 10, but can be significantly lower for higher N.

The damping ratio for D_r=80% lies between the mean and the lower Seed-Idriss (1970) curves for N=1 and is similar to or higher than the damping ratio for D_r=100%. The damping ratio for D_r=80% and N=10 is, however, significantly lower than the lower Seed-Idriss (1970) curve and the N=10 curve for D_r=100%.

5.1.2 Effect of overconsolidation ratio on damping ratio in DSS tests on sand

The damping ratio for overconsolidated (OCR=4) and normally consolidated sand with D_r=80% is compared in Figure 5.4. The shape of the damping curves from the individual

tests is similar, but the damping ratio has a tendency to be lower for overconsolidated than for normally consolidated sand at low N (N=1 to 10).

5.1.3 Effect of consolidation stress on damping ratio in DSS tests on sand

The damping ratio for tests with low consolidation stress (40 kPa) is compared to the damping ratio for tests with consolidation stress of 200 kPa in Figures 5.5-5.7. The shape of the damping curves from the individual tests is similar, but the damping ratio has some tendency to increase with decreasing consolidation stress, especially for overconsolidated sand with D_r=80%. However, one should keep in mind that the number of tests with low consolidation stress is limited with only one test with overconsolidated sand with D_r=80%.

5.1.4 Effect of precycling on damping ratio in DSS tests on sand

The damping ratio for tests with and without precycling is compared in Figures 5.8, 5.9 and 5.10. The shape of the damping curves from the individual tests is similar, and precycling does not seem to have effect on the damping ratio for D_r=100%. For D_r=80%, the damping ratio seems to be the same for N=1, but precycling seems to give higher damping ratio for N=10 to 30. This difference may be due to scatter in the results, since there are few test with precycling.

5.1.5 Effect of average shear stress on damping ratio in DSS tests on sand

The damping ratio for tests with and without an average shear stress, τ_a, during cycling is compared in Figures 5.11, 5.12 and 5.13. The average shear stress was applied drained in some tests and undrained in others.

There is some tendency that τ_a>0 may give lower damping ratio than tests with τ_a=0 for sand with D_r=80% for small N, and the damping ratio may be smaller for undrained than for drained τ_a. The damping ratio is higher for tests with τ_a>0 than for tests with τ_a=0 when N>10.

The damping ratio is less influenced by τ_a for D_r=100% and low N. There is some tendency for the damping ratio to be smaller for tests with τ_a>0 than for tests with τ_a=0 at N=10 and higher.

5.1.6 Effect of fines content on damping ratio in DSS tests on sand

The damping ratio for tests on sand with 20% fines content (Sand B) is compared to sand with no fines (Sand A) in Figures 5.14, 5.15 and 5.16. The damping ratio seems to

decrease with increasing fines content, but the effect is less clear for D_r=80% than for D_r=100%.

5.2 Damping ratio in triaxial tests on sand

As in the DSS tests, the damping ratio in triaxial tests on dense sand depends on both cyclic shear strain and number of cycles, as seen in Figures 5.17 and 5.18. However, the shape of the curves for the individual tests is different in triaxial and DSS tests. In the DSS tests the damping ratio increases with cyclic shear strain during the first cycles, reaches a maximum value and starts to decrease with increasing shear strains (e.g. Figures 5.1 and 5.2). The increase in damping ratio during the first cycles is less pronounced or negligible in the triaxial tests (e.g. Figures 5.17 and 5.18). The exception is the overconsolidated sand (e.g. Figure 5.20). The damping ratio in DSS and triaxial tests is compared in Figures 5.36 to 5.40.

The reason for the difference between triaxial and DSS tests during the first cycles may be that the triaxial tests on normally consolidated sand cycle around an average shear stress, whereas the DSS tests and the triaxial tests on overconsolidated clay cycle around zero average shear stress.

5.2.1 Effect of density on damping ratio in triaxial tests on sand

The damping ratio for clean sand with relative density of 100% and 80% is presented in Figures 5.17 and 5.18 and compared in Figure 5.19.

The damping ratio for D_r=100% is close to the mean Seed-Idriss (1970) curve for N=1 and close to the lower Seed-Idriss (1970) curve for N=10. It can be significantly lower for higher N.

The damping ratio for D_r=80% tends to be somewhat higher than for D_r=100% at low N.

5.2.2 Effect of overconsolidation ratio on damping ratio in triaxial tests on sand

The damping ratio for overconsolidated (OCR=4) and normally consolidated sand with D_r=80% is compared in Figure 5.20. The shape of the damping curves from the individual tests are different, with a tendency for a peak in the curves for two of the three tests the overconsolidated sand.

The damping ratio as function of cyclic shear strain seems less dependent of N for overconsolidated than for normally consolidated sand, with damping ratio for overconsolidated sand being lower at low N (N=1 to 10).

5.2.3 Effect of consolidation stress on damping ratio in triaxial tests on sand

The damping ratio for tests with low consolidation stress (40 kPa) is compared to the damping ratio for tests with 200 kPa consolidation stress in Figures 5.21, 5.22 and 5.23. The damping ratio is highest in the test with lowest consolidation stress in the test on overconsolidated sand with D_r=80%. However, this is based on only one test, and there is no clear effect of consolidation stress in normally consolidated sand with D_r=100% and D_r=80%.

5.2.4 Effect of precycling on damping ratio in triaxial tests on sand

The damping ratio for tests with and without precycling is compared in Figures 5.24, 5.25 and 5.26. The shape of the damping curves from the individual tests is similar. Precycling does not seem to have effect on the damping ratio for N≤10, but the damping ratio becomes higher for tests with precycling when N>10.

5.2.5 Effect of average shear stress on damping ratio in triaxial tests on sand

The damping ratio for tests with and without an average shear stress, τ_a, different from the shear stress during consolidation, τ_0, is compared in Figures 5.27, 5.28, 5.29, 5.30 and 5.31. The additional shear stress, $\Delta\tau_a = \tau_a - \tau_0$, was applied drained in some tests and undrained in other.

There is no clear effect of average shear stress, τ_a, different from τ_0, on the damping ratio, neither for drained nor undrained $\Delta\tau_a$.

5.2.6 Effect of fines content on damping ratio in triaxial tests on sand

The damping ratio for tests on sand with 20% fines content (Sand B) is compared to sand with no fines (Sand A) in Figures 5.32, 5.33, 5.34 and 5.35.

The damping ratio does not seem to be influenced by increasing fines content.

5.3 Comparison of damping ratio in DSS and triaxial tests on sand

The damping ratio in DSS and triaxial tests is compared in Figures 5.36, 5.37, 5.38, 5.39 and 5.40 for clean sand, sand with 20% fines, Dr=100%, D_r=80% and OCR=4.

The comparisons show a difference in the shape of the damping ratio vs. cyclic shear strain for individual tests between DSS and triaxial tests. This was discussed in the

beginning of Section 5.2. On sand with D_r=80% (Figure 5.40), the damping ratio is higher in the triaxial than in the DSS tests for N=1 and tends to be lower for higher N.

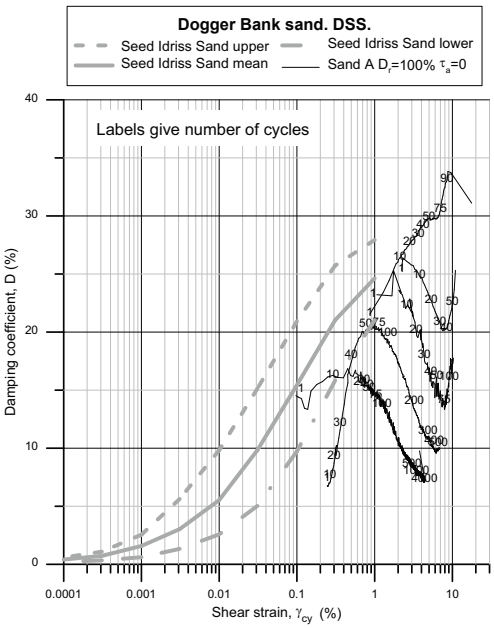

Figure 5.1 Damping ratio as function of cyclic shear strain in DSS tests on clean sand with D_r=100%. Symmetrical cyclic loading.

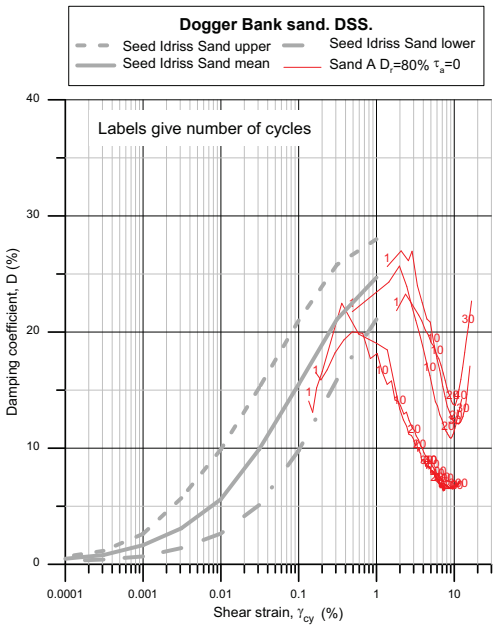

Figure 5.2 Damping ratio as function of cyclic shear strain in DSS tests on clean sand with D_r=80%. Symmetrical cyclic loading.

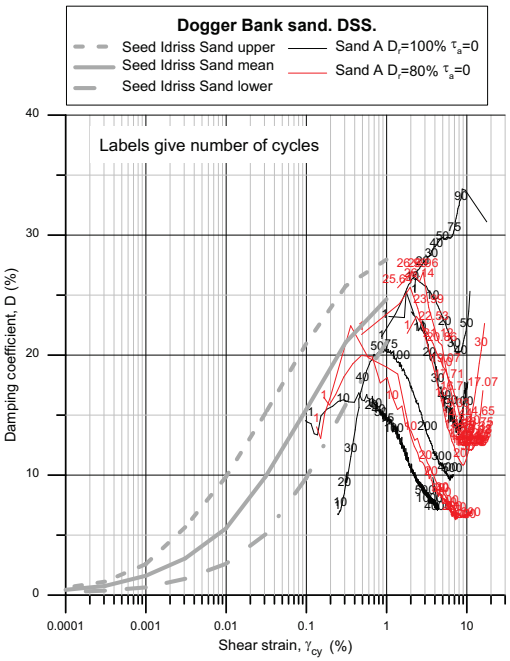

Figure 5.3 Comparison of damping ratio in DSS tests on clean sand with D_r=80% and 100%. Symmetrical cyclic loading.

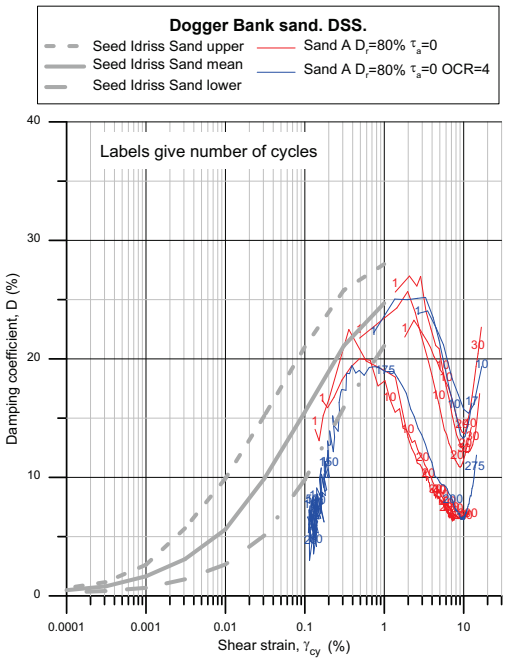

Figure 5.4 Effect of overconsolidation ratio on damping ratio in DSS tests on clean sand with D_r=80%. Symmetrical cyclic loading.

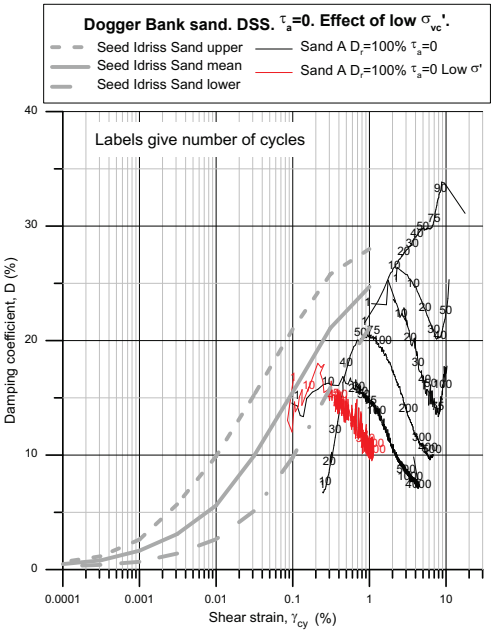

Figure 5.5 Effect of consolidation stress on damping ratio in DSS tests on clean sand with D_r=100%. Symmetrical cyclic loading.

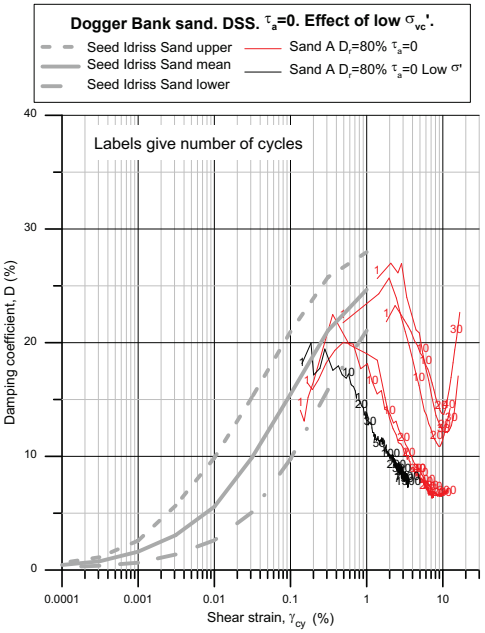

Figure 5.6 Effect of consolidation stress on damping ratio in DSS tests on clean sand with D_r=80%. Symmetrical cyclic loading.

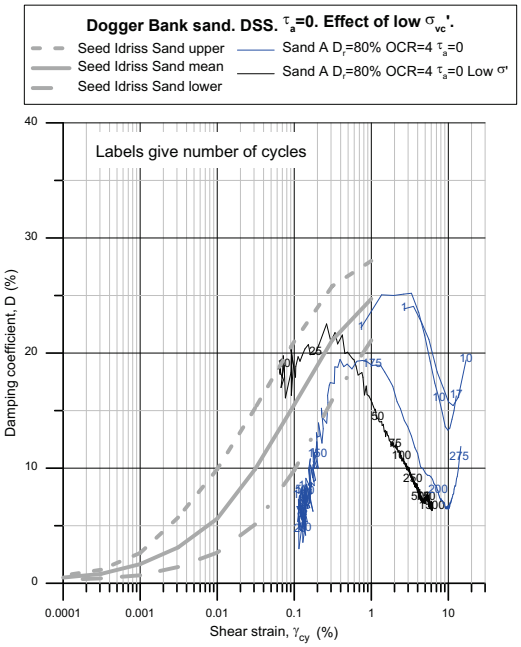

Figure 5.7 Effect of consolidation stress on damping ratio in DSS tests on clean sand with D_r=80% and OCR=4. Symmetrical cyclic loading.

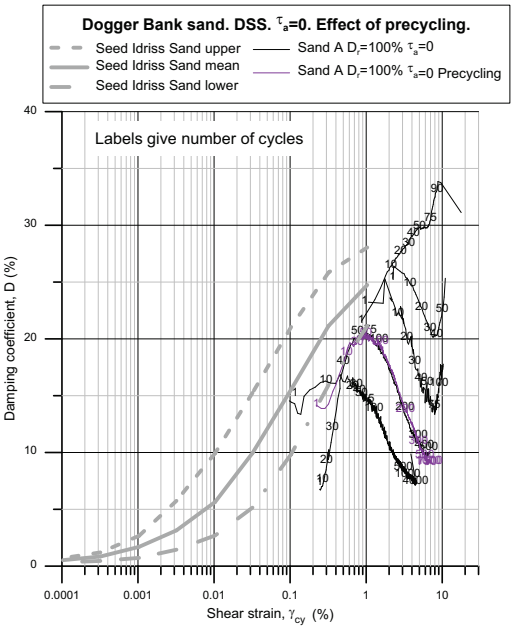

Figure 5.8 Effect of precycling on damping ratio in DSS tests on clean sand with D_r=100%. Symmetrical cyclic loading.

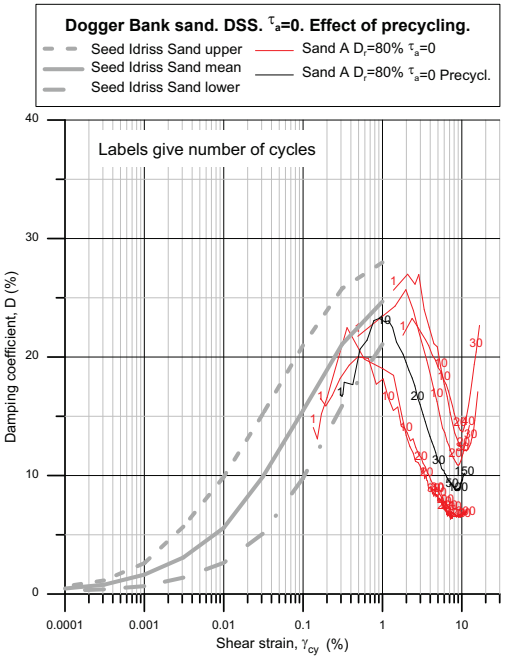

Figure 5.9 Effect of precycling on damping ratio in DSS tests on clean sand with D_r=80%. Symmetrical cyclic loading.

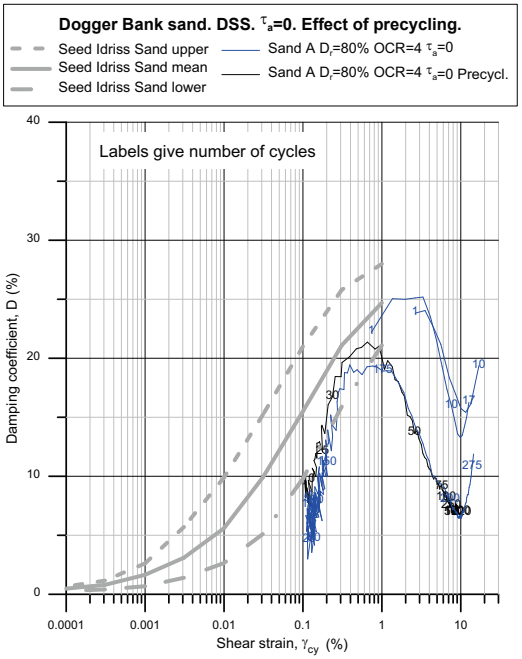

Figure 5.10 Effect of precycling on damping ratio in DSS tests on clean sand with D_r=80% and OCR=4. Symmetrical cyclic loading.

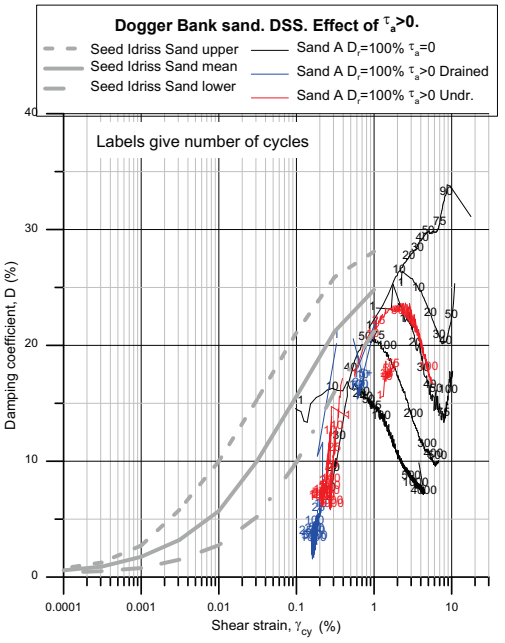

Figure 5.11 Effect of average shear stress on damping ratio in DSS tests on clean sand with D_r=100%.

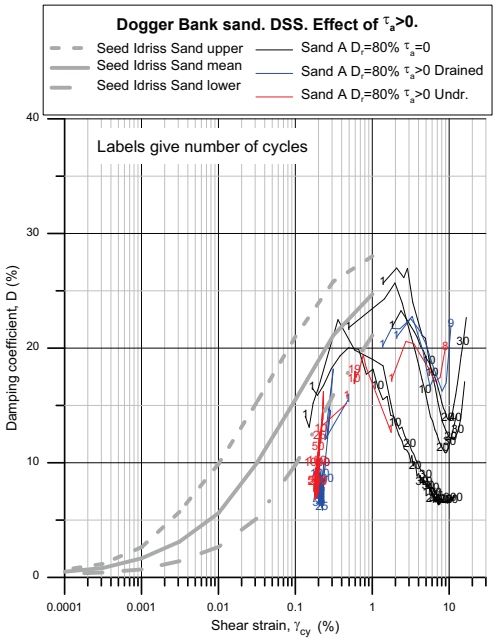

Figure 5.12 Effect of average shear stress on damping ratio in DSS tests on clean sand with D_r=80%.

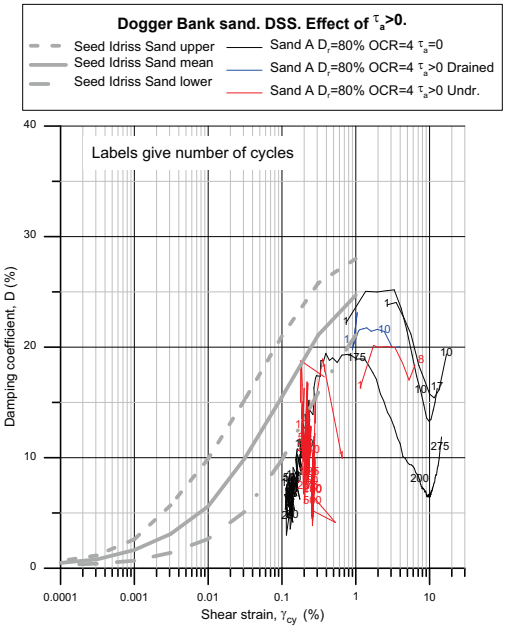

Figure 5.13 Effect of average shear stress on damping ratio in DSS tests on clean sand with D_r=80% and OCR=4.

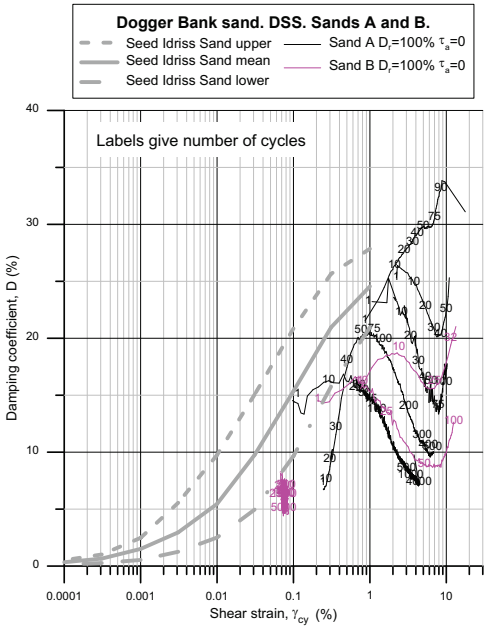

Figure 5.14 Comparison of damping ratio in DSS tests with D_r=100% on clean sand and sand with 20% fines. Symmetrical cyclic loading.

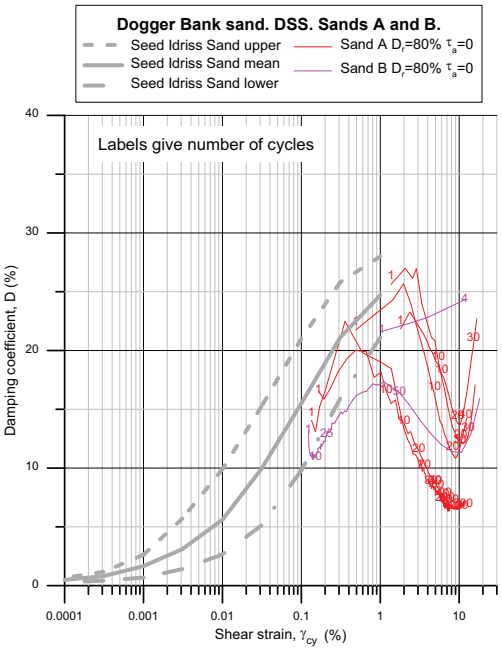

Figure 5.15 Comparison of damping ratio in DSS tests with D_r=80% on clean sand and sand with 20% fines. Symmetrical cyclic loading.

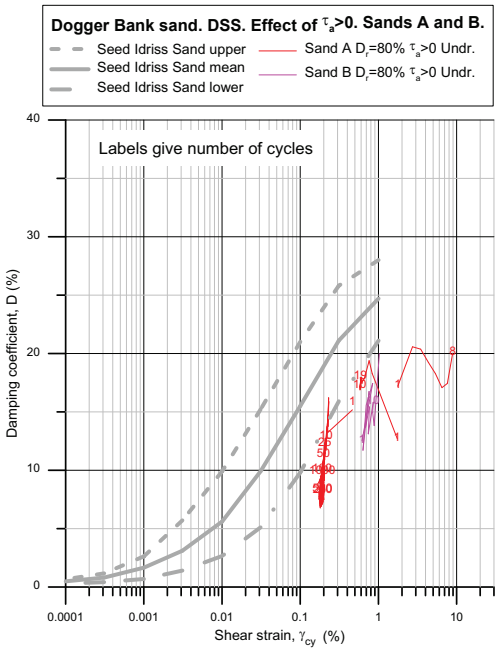

Figure 5.16 Comparison of damping ratio in DSS tests with D_r=80% on clean sand and sand with 20% fines. Non-symmetrical cyclic loading.

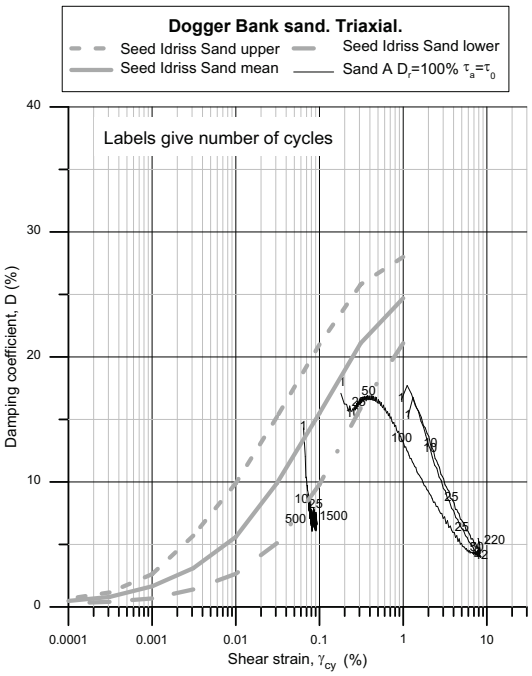

Figure 5.17 Damping ratio as function of cyclic shear strain in triaxial tests on clean sand with D_r=100%. $\tau_a = \tau_0$.

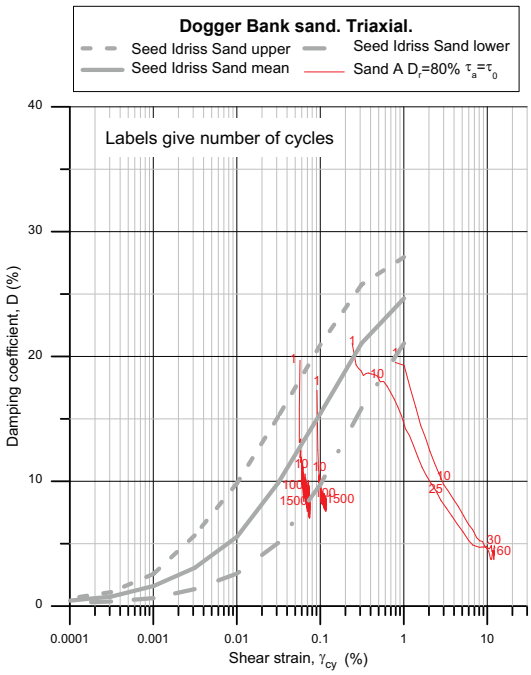

Figure 5.18 Damping ratio as function of cyclic shear strain in triaxial tests on clean sand with D_r=80%. $\tau_a = \tau_0$.

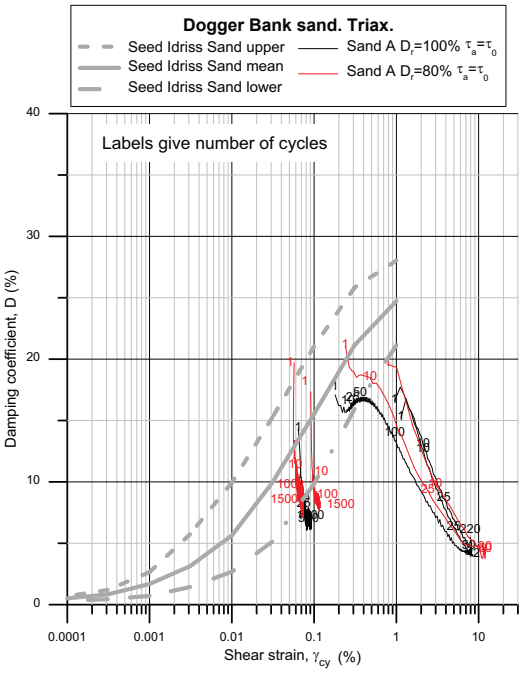

Figure 5.19 Comparison of damping ratio in triaxial tests on clean sand with D_r=80% and 100%. $\tau_a = \tau_0$.

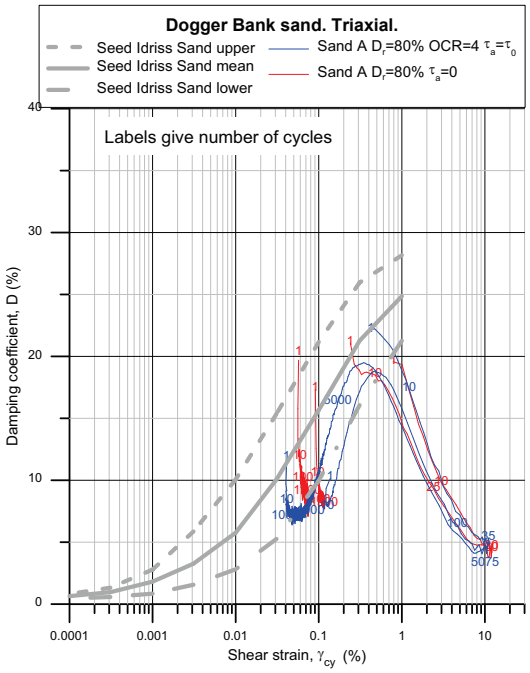

Figure 5.20 Effect of overconsolidation ratio on damping ratio in triaxial tests on clean sand with D_r=80%. $\tau_a = \tau_0$.

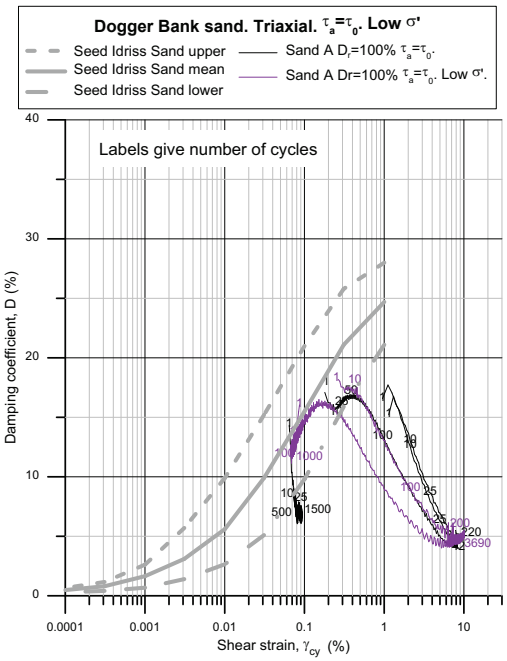

Figure 5.21 Effect of consolidation stress on damping ratio in triaxial tests on clean sand with D_r=100%. $\tau_a = \tau_0$.

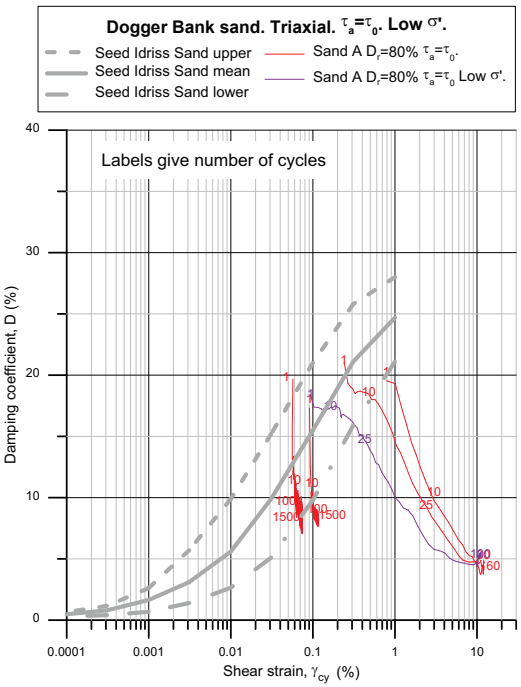

Figure 5.22 Effect of consolidation stress on damping ratio in triaxial tests on clean sand with D_r=80%. $\tau_a = \tau_0$.

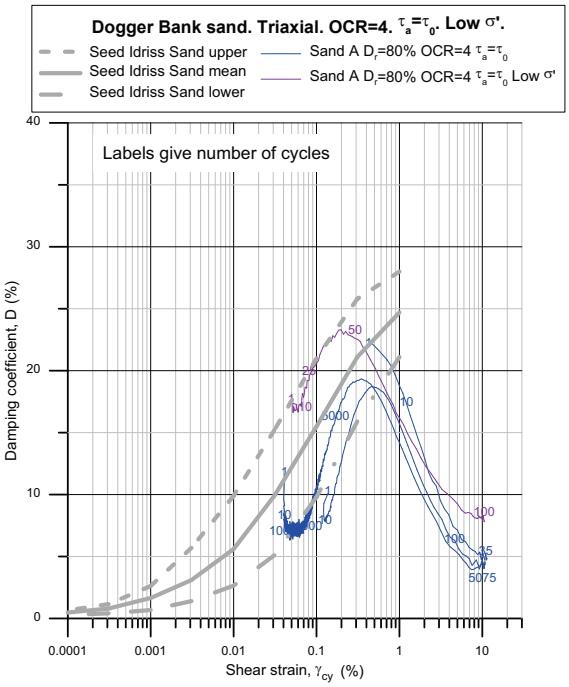

Figure 5.23 Effect of consolidation stress on damping ratio in triaxial tests on clean sand with D_r=80% and OCR=4. $\tau_a = \tau_0$.

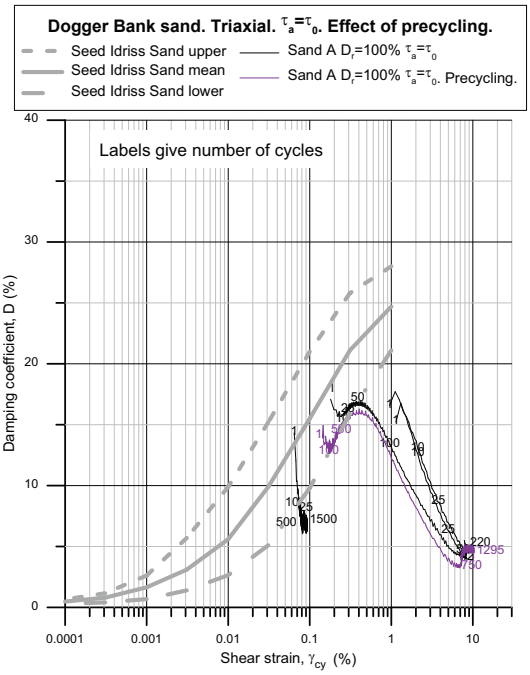

Figure 5.24 Effect of precycling on damping ratio in triaxial tests on clean sand with D_r=100%. $\tau_a = \tau_0$.

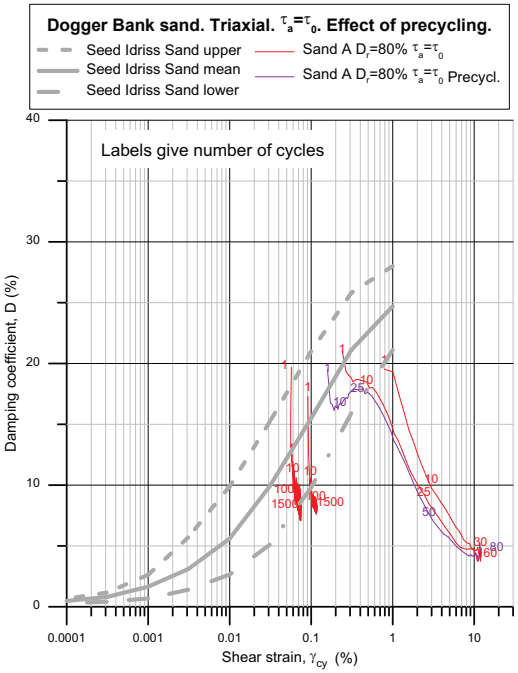

Figure 5.25 Effect of precycling on damping ratio in triaxial tests on clean sand with D_r=80%. $\tau_a=\tau_0$.

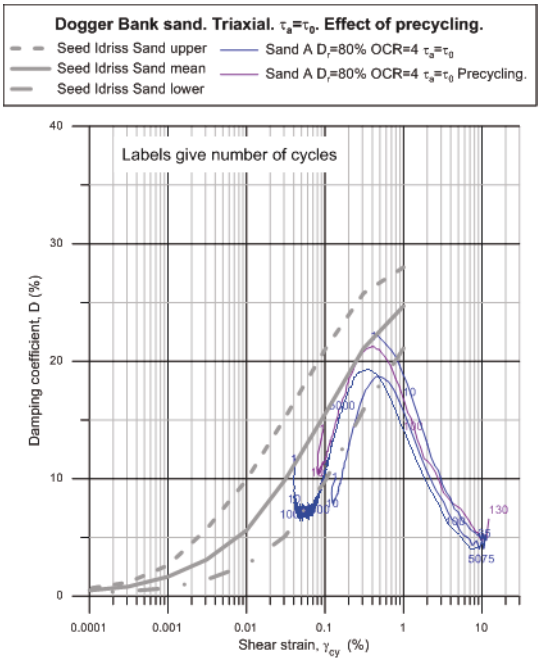

Figure 5.26 Effect of precycling on damping ratio in triaxial tests on clean sand with D_r=80% and OCR=4. $\tau_a=\tau_0$.

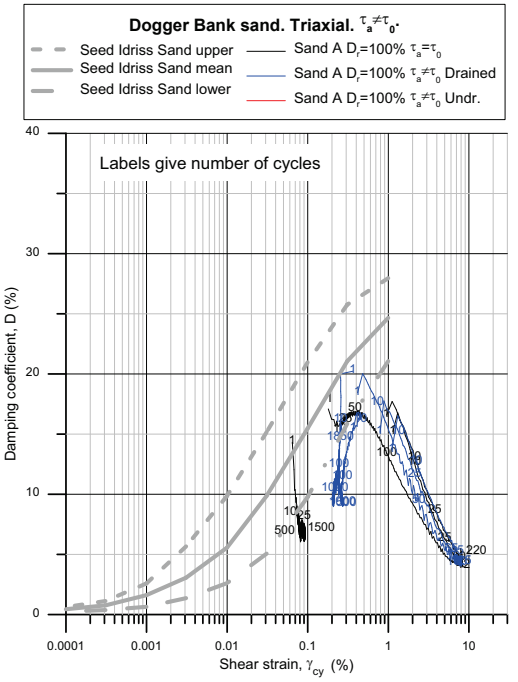

Figure 5.27 Effect of drained average shear stress on damping ratio in triaxial tests on clean sand with D_r=100%.

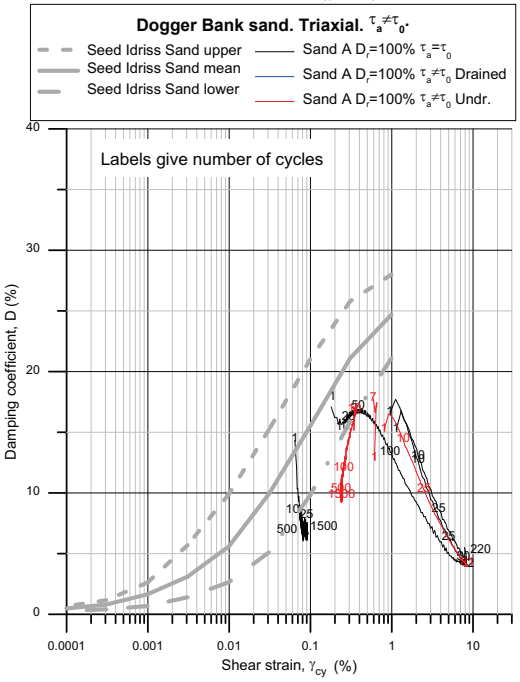

Figure 5.28 Effect of undrained average shear stress on damping ratio in triaxial tests on clean sand with D_r=100%.

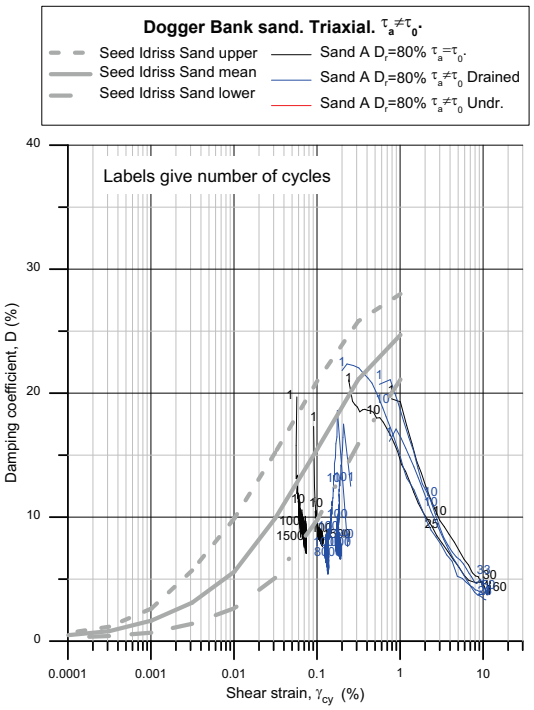

Figure 5.29 Effect of drained average shear stress on damping ratio in triaxial tests on clean sand with D_r=80%.

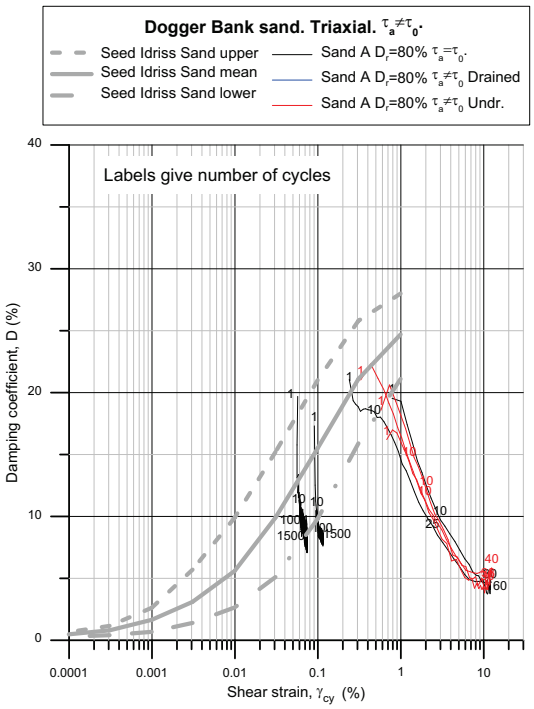

Figure 5.30 Effect of undrained average shear stress on damping ratio in triaxial tests on clean sand with D_r=80%.

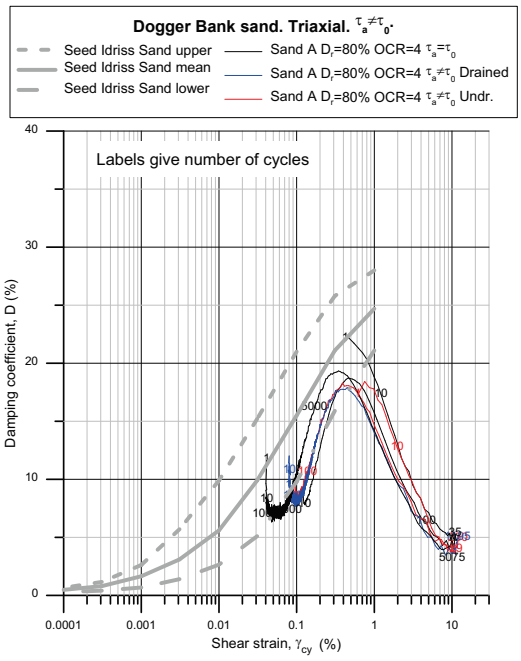

Figure 5.31 Effect of average shear stress on damping ratio in triaxial tests on clean sand with D_r=80% and OCR=4.

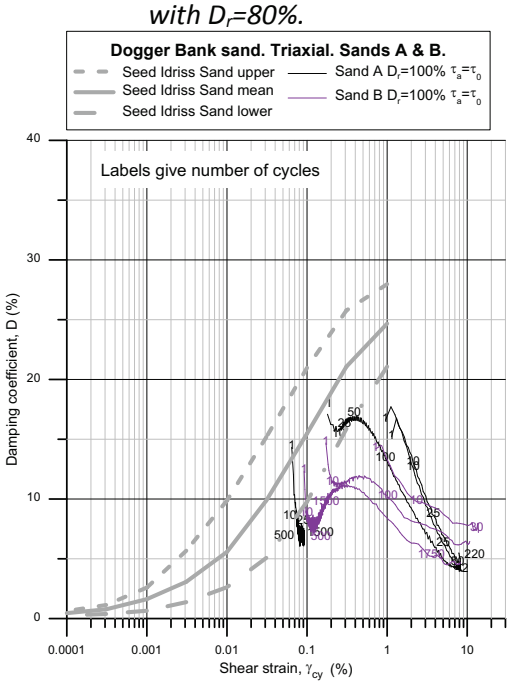

Figure 5.32 Comparison of damping ratio in triaxial tests with D_r=100% on clean sand and sand with 20% fines. $\tau_a = \tau_0$.

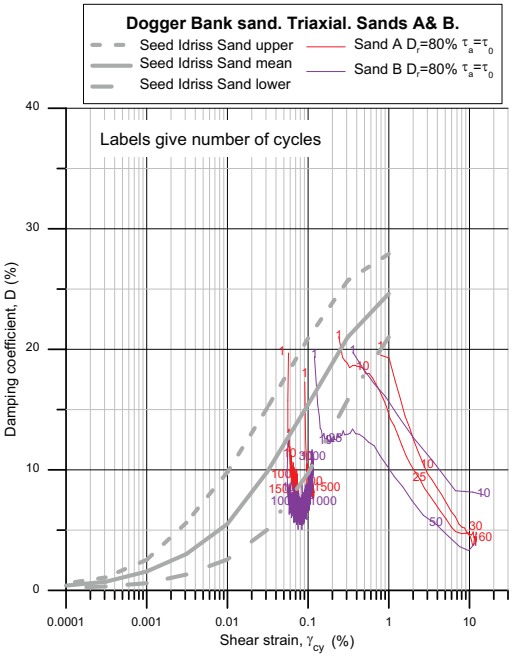

Figure 5.33 Comparison of damping ratio in triaxial tests with D_r=80% on clean sand and sand with 20% fines. $\tau_a = \tau_0$.

Figure 5.34 Comparison of damping ratio in triaxial tests with D_r=80% on clean sand and sand with 20% fines $\tau_a \neq \tau_0$.

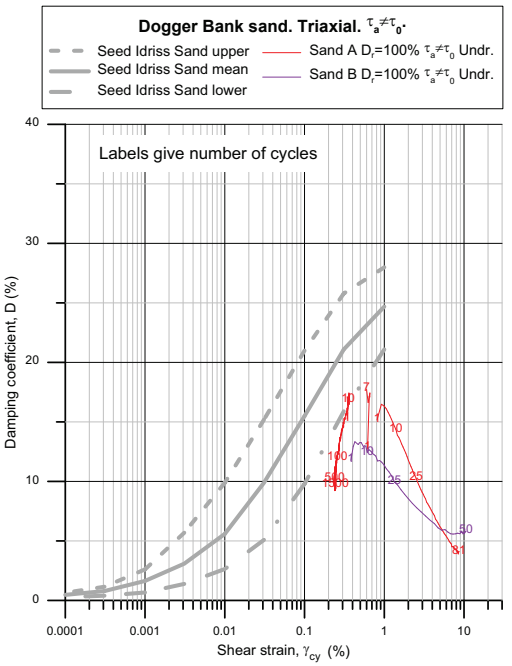

Figure 5.35 Comparison of damping ratio in triaxial tests with D_r=100% on clean sand and sand with 20% fines. $\tau_a \neq \tau_0$.

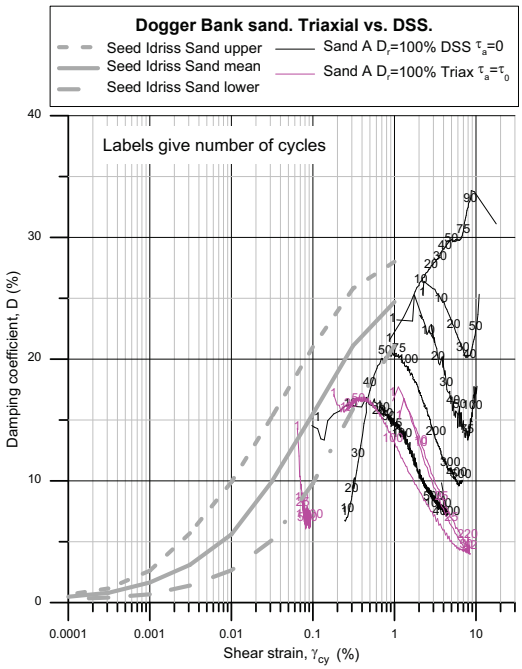

Figure 5.36 Comparison of damping ratio in DSS (τ_a=0) and triaxial tests $\tau_a = \tau_0$) on clean sand with D_r=100%.

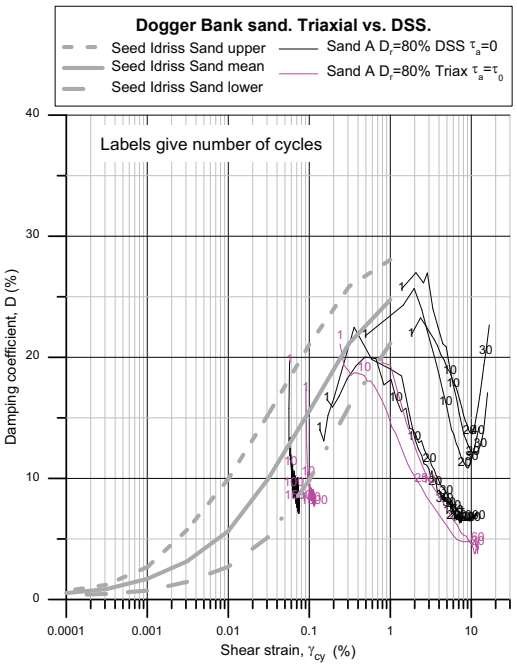

Figure 5.37 Comparison of damping ratio in DSS ($\tau_a = \tau_0 = 0$) and triaxial tests ($\tau_a = \tau_0$) on clean sand with D_r=80%.

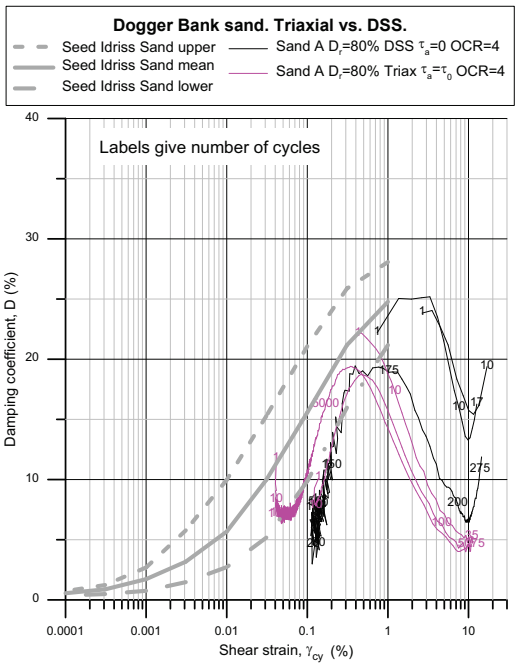

Figure 5.38 Comparison of damping ratio in DSS ($\tau_a = 0$) and triaxial tests ($\tau_a = \tau_0$) on clean sand with D_r=80% and OCR=4.

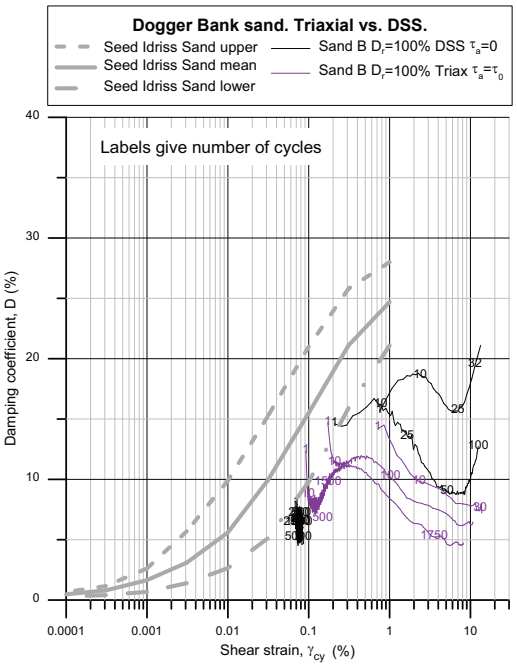

Figure 5.39 Comparison of damping ratio in DSS ($\tau_a = 0$) and triaxial tests ($\tau_a = \tau_0$) on sand with 20% fines and D_r=100%.

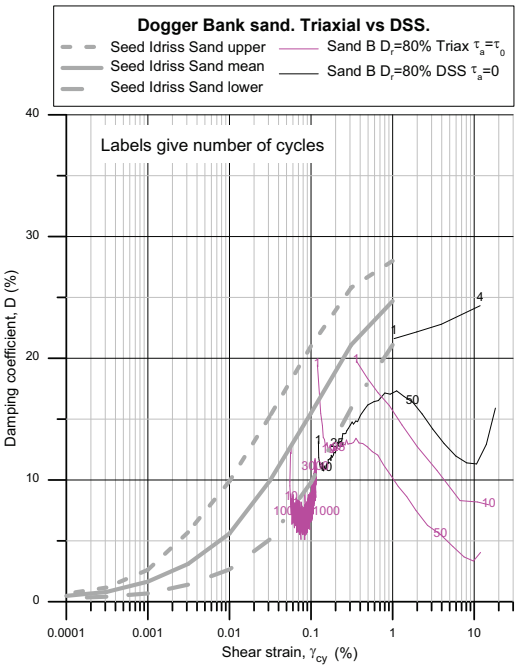

Figure 5.40 Comparison of damping ratio in DSS ($\tau_a = 0$) and triaxial tests ($\tau_a = \tau_0$) on sand with 20% fines and D_r=80%.

6 Comparison with literature

6.1 Comparison with Seed and Idriss (1970)

Seed and Idriss (1970) present mean, as well as upper and lower curves of damping ratio as functions of cyclic shear strain for clays and sands. It is not specifically stated, but the data are most likely based on symmetrically loaded strain controlled tests. No guidance is given for non-symmetrical cyclic loading or for triaxial type loading.

Seed and Idriss (1970) state that the damping ratio for sand depends on shear strain, octahedral effective normal stress, number of cycles and void ratio. The grain size distribution is said to be less important. The curves they present for sand is valid for 5 to 10 cycles and an octahedral effective normal stress of about 290 to 435 kPa. No guidance is given with respect to effect of void ratio. Five to ten cycles may be representative for earthquake analyses, but for other cases, like fatigue for wind power structures, a higher number of cycles may be more relevant. Seed-Idriss (1970) present a formula indicating that the damping ratio may decrease by about 10% as the number of cycles increases from 10 to 1000.

Seed and Idriss (1970) state that their curves for clay are based on less data than for sand, and they do not identify what parameters the damping ratio for clay may depend on.

The damping ratio from the tests reported herein was compared to the damping ratio curves proposed by Seed and Idriss (1970) in the figures in Sections 4 and 5 and discussed in the text. In general, the comparisons showed that:

- for clay, the range in damping ratio between upper and lower Seed and Idriss (1970) curves is quite significant, and the damping ratio of the three clays generally falls within the upper and lower curves from Seed-Idriss (1970). However, the damping ratio for the high plasticity clay and the quick clay are below the mean Seed-Idriss (1970) curve, and even below the lower Seed-Idriss (1970) curve at large cyclic shear strains (γ_{cy} >2%).
- for sand
  - the range in damping ratio between upper and lower Seed and Idriss (1970) curves is also significant. The damping ratio for sand with D_r=100% is between the lower and the mean Seed-Idriss (1970) curves for N=1 to about 10, but can be significantly lower for higher N. The effect of N is more significant in the tests than indicated by the formula in Seed and Idriss (1970).
  - The damping ratio is similar to, or somewhat higher for D_r=80% than for D_r=100% for low N (N=1 to 3). The damping ratio in DSS tests on sand with D_r=80% and N=10 is, however, significantly lower than the lower Seed-Idriss (1970) curve and the N=10 curve for D_r=100%.

6.2 Comparison with Darendeli (2001)

Darendeli (2001) presents curves of damping ratio as function of cyclic shear strain as function of plasticity index, consolidation stress, overconsolidation ratio, load period and number of cycles. The curves are based on combined resonant column and torsional shear laboratory tests with symmetrical cyclic loading. No guidance is given for non-symmetrical cyclic loading or for triaxial type loading.

The damping ratio curves in the figures in this report are determined with a spread sheet prepared by Dr. Jørgen Johansson, NGI.

The Darendeli (2001) damping curves are compared to the damping ratio from the tests reported herein in the following two subsections.

6.2.1 Clay

Comparisons between test results and the Darendeli (2001) curves are presented in Figures 6.1 to 6.3 for the high plasticity clay, the low plasticity clay and the quick clay, respectively. A summary of the comparisons is given in Table 6.1.

Table 6.1 Darendeli (2001) damping ratio curves compared to test results. Clays.

Cyclic strain range	**Small (γ_{cy} <0.5%)**	**Intermediate (γ_{cy}=0.5% - 3%)**	**High (γ_{cy}>3%)**
High I_p	Low? *	Close	Low
Low I_p	Low for N≤10		Low
Quick clay	Low	High	Low

** No test data*

The Darendeli (2001) curves generally give lower damping ratio than the test data at small (<0.3%) and high (>3%) cyclic shear strains. At intermediate strains, the Darendeli (2001) curves give similar, lower, and higher damping ratio than measured for high plasticity, low plasticity and quick clays, respectively.

The effect of load period in the Darendeli (2001) expression at low γ_{cy} can be questioned, as it gives a negative damping ratio for a 100s load period (Figure 6.1). It seems that the effect of load period may be underestimated at higher γ_{cy} (Figure 6.1).

The Darendeli (2001) curves show smaller effect of number of cycles than what the test results for quick clay and, to some extent, the high plasticity clay seem to indicate.

6.2.2 Sand

Comparisons between test results and the Darendeli (2001) curves are presented in Figures 6.4 to 6.11 for clean sand with D_r=100% and 80%, respectively. A summary of the comparisons is given in Table 6.1.

Table 6.2 Darendeli (2001) damping ratio curves compared to test results. Sands.

Cyclic strain range	Small (γ_{cy} <0.1%)	Intermediate (γ_{cy}=0.1% - 1%)	High (γ_{cy}>1%)
Clean sand D_r=100%	No test data	Close for N<10 High for N>10	Low for N<25 High for N>25
Clean sand D_r=80%		Close for N<5 High for N>5	Low for N<5 High for N>5
Clean sand D_r=80% OCR=4		Close for N<5 High for N>5	Low for N<5 High for N>5
Clean sand D_r=100% Low σ_{vc}'		Similar effect of σ_{vc}'	-
Clean sand D_r=80% Low σ_{vc}'		Similar effect of σ_{vc}'	-
Clean sand D_r=80% OCR=4 Low σ_{vc}'		Smaller effect of σ_{vc}'	-
Sand w. 20% fines D_r=100%		Close for N=1 High for N>1	Low for N<5 High for N>5
Sand w. 20% fines D_r=80%		Close for N=1 High for N>1	Low for N<5 High for N>5

The Darendeli (2001) curves

- do not reflect the large effect of N seen in the tests on dense sand
- overestimate the damping ratio for high N. This is important to note for fatigue analyses where the number of representative cycles can be high
- generally give damping ratio close to measured in the intermediate strain range (γ_{cy} =0.1% - 1%) for clean sand for N<5, but overestimate the damping ratio for N>5. The same is true for the sand with 20% fines, but for N=1 instead of N=5.
- give reasonable agreement with the tests in the high strain range (γ_{cy} >1%) for N=25 in the clean sand with Dr=100% and for N=5 for clean sand with Dr=80% and for the sand with 20% fines. The damping ratio is underestimated for lower N and overestimated for higher N.
- predict similar effect of σ_{vc}' as seen in the tests
- predict no effect of overconsolidation ratio, which agrees with only a small tendency for the damping ratio to decrease with increasing overconsolidation ratio (Section 5.1.2 and Figure 5.4).

There are no test data at low cyclic shear strain, and no conclusion is drawn about the agreement between the Darendeli (2001) curves and the test data for γ_{cy} <0.1%.

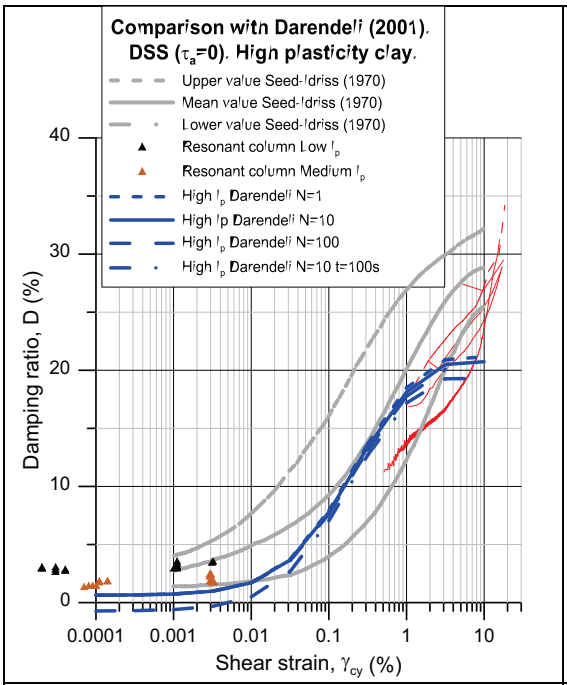

Figure 6.1 Comparison of Darendeli (2001) with test data. DSS tests with τ_a =0 on high plasticity clay.

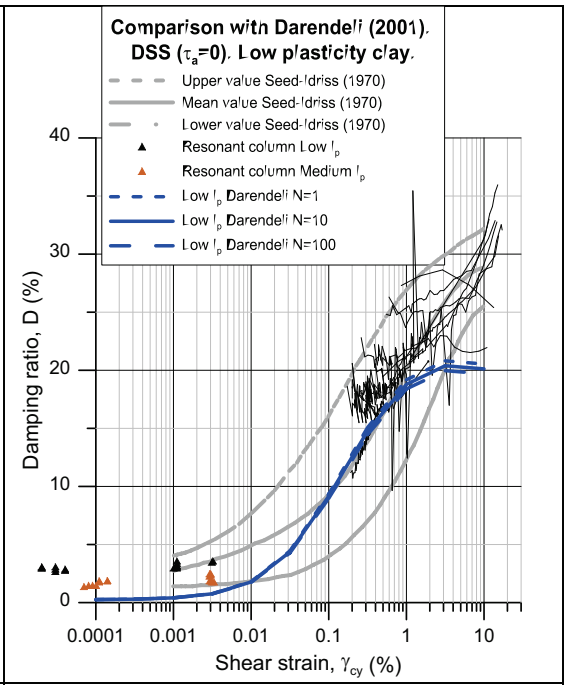

Figure 6.2 Comparison of Darendeli (2001) with test data. DSS tests with τ_a =0 on low plasticity clay.

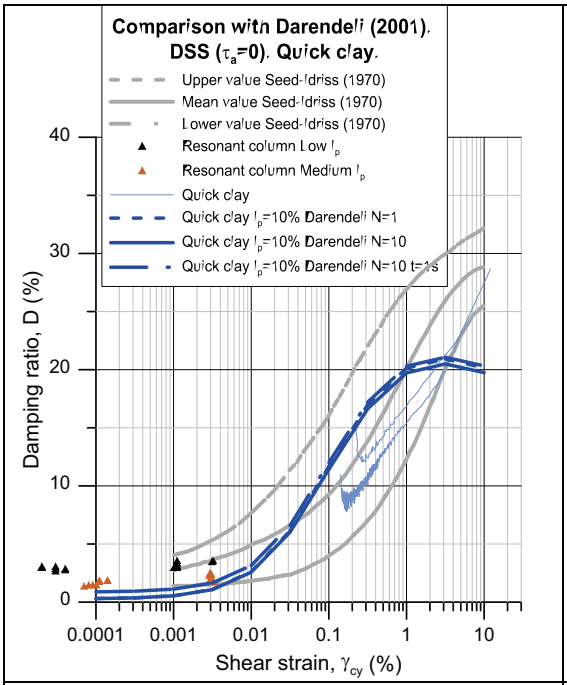

Figure 6.3 Comparison of Darendeli (2001) with test data. DSS tests with τ_a =0 on clean sand with D_r=100%.

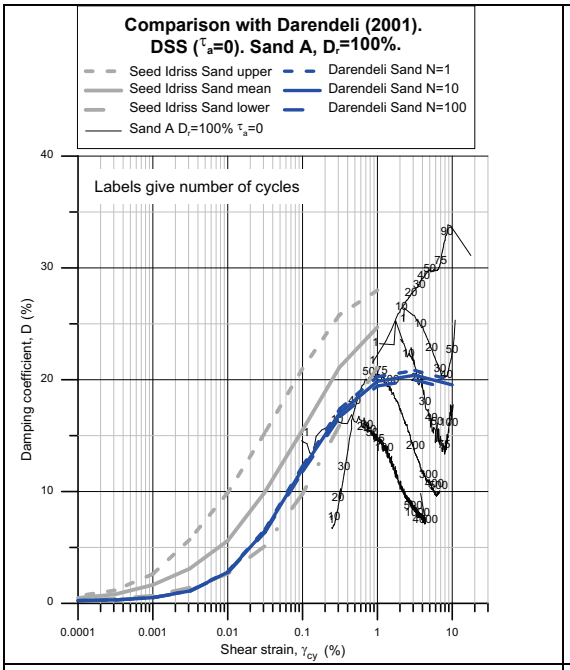

Figure 6.4 Comparison of Darendeli (2001) with test data. DSS tests with τ_a =0 on clean sand with D_r=100%.

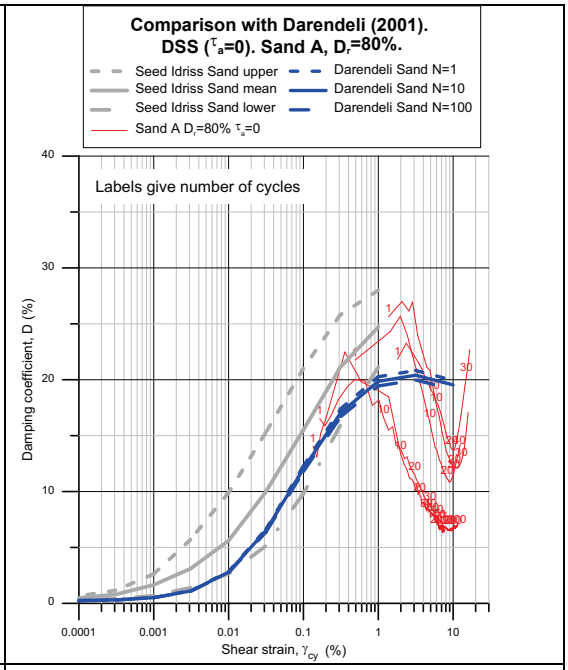

Figure 6.5 Comparison of Darendeli (2001) with test data. DSS tests with τ_a =0 on clean sand with D_r=80%.

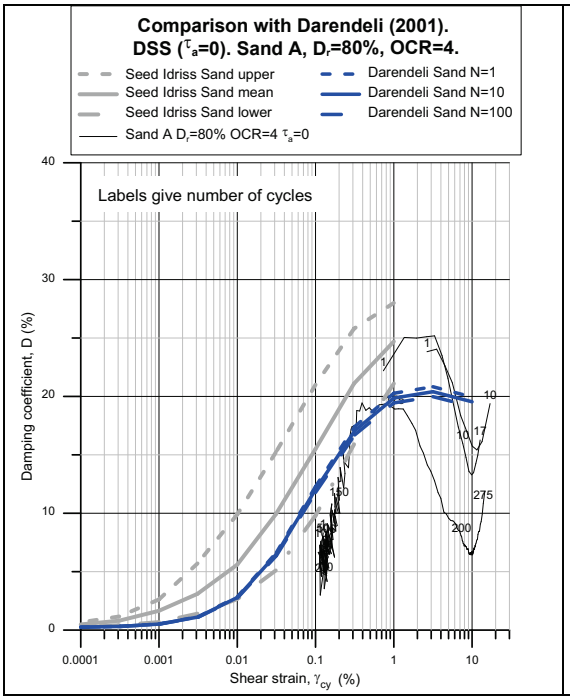

Figure 6.6 Comparison of Darendeli (2001) with test data. DSS tests with τ_a =0 on clean sand with D_r=80% and OCR=4.

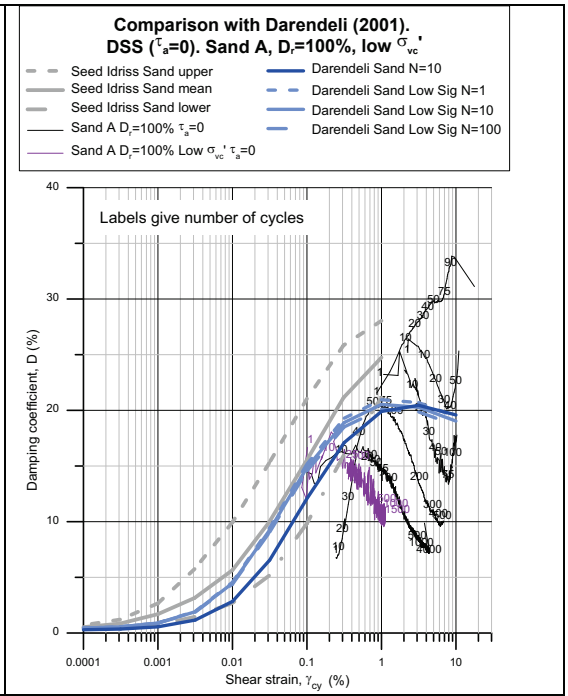

Figure 6.7 Comparison of Darendeli (2001) with test data. DSS tests with τ_a =0 on clean sand with D_r=100%. Low σ_{vc}'.

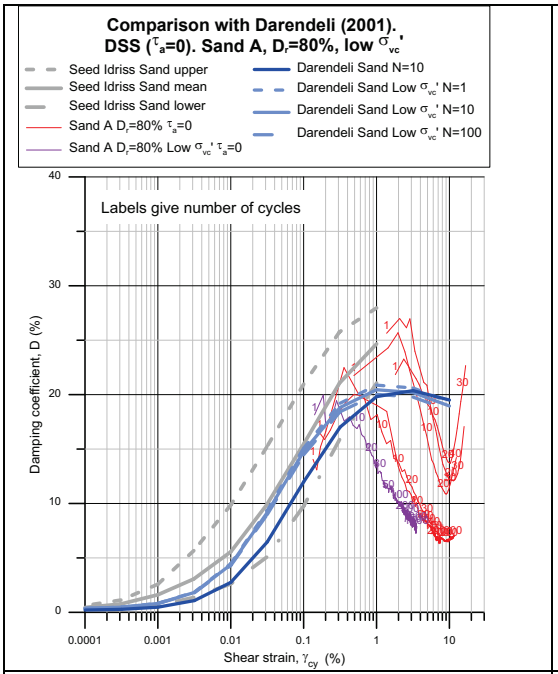

Figure 6.8 Comparison of Darendeli (2001) with test data. DSS tests with τ_a =0. Clean sand, D_r=80% and low σ_{vc}'.

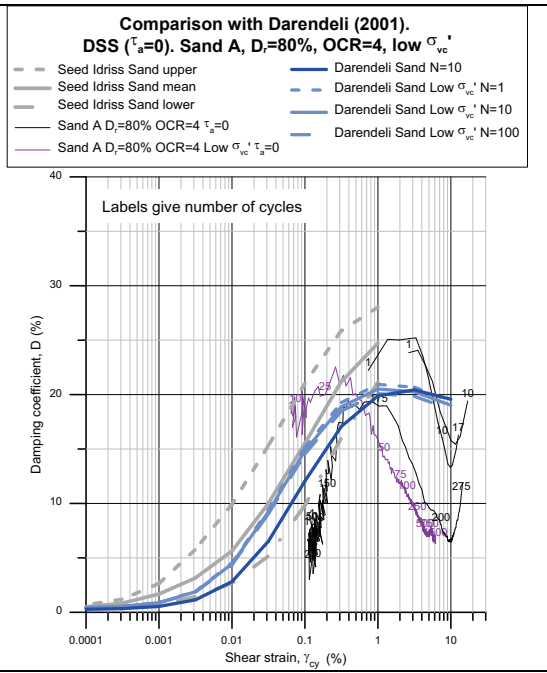

Figure 6.9 Comparison of Darendeli (2001) with test data. DSS tests with τ_a =0. Clean sand, D_r=80%, OCR=4, low σ_{vc}'.

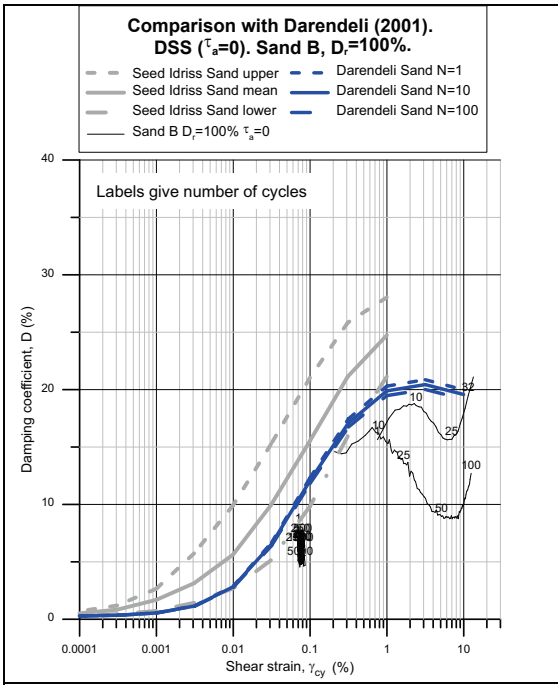

Figure 6.10 Comparison of Darendeli (2001) with test data. DSS tests with τ_a =0 on sand with 20% fines and D_r=100%.

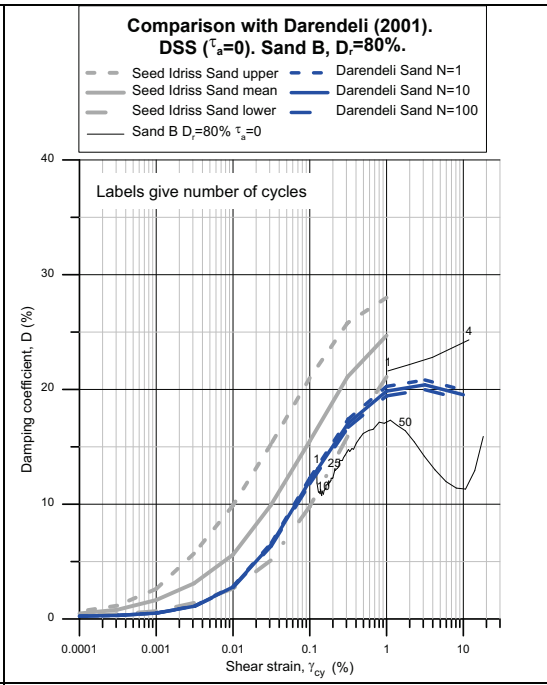

Figure 6.11 Comparison of Darendeli (2001) with test data. DSS tests with τ_a =0 on sand with 20% fines and D_r=80%.

7 References

Blaker, Ø. and Andersen, K.H. (2015) Shear strength of dense to very dense Dogger Bank sand. *Frontiers in Offshore Geotechnics III, ISFOG'2015, Meyer (Ed).* Taylor & Francis Group, London, ISBN: 978-1-138-02848-7. Proc., 1167-1172.

Darendeli M.B. (2001) development of a new family of normalized modulus reduction and material damping curves. Ph.D. dissertation, University of Texas at Austin, August 2001.

NGI (2014) Estimation of hysteretic soil damping from laboratory measurements including strain accumulation. *NGI report 20110087-01-R*.

Seed, H.B. and Idriss, I.M. (1970) Soil moduli and damping factors for dynamic response analyses. *Earthquake Engineering Research Center. Report No. EERC 70-10, December 1979.*

Kontroll- og referanseside/ Review and reference page

Dokumentinformasjon/*Document information*		
Dokumenttittel/*Document title* Damping ratio from laboratory tests		**Dokumentnr./*Document no.*** 20150014-01-R
Dokumenttype/*Type of document* Rapport / Report	**Oppdragsgiver/*Client*** Research Council oF Norway	**Dato/*Date*** 2016-06-02
Rettigheter til dokumentet iht kontrakt/ *Proprietary rights to the document according to contract* NGI		**Rev.nr.&dato/*Rev.no.&date*** 0
Distribusjon/*Distribution* FRI: Kan distribueres av Dokumentsenteret ved henvendelser / FREE: Can be distributed by the Document Centre on request		
Emneord/*Keywords*		

Stedfesting/*Geographical information*	
Land, fylke/*Country*	**Havområde/*Offshore area***
Kommune/*Municipality*	**Feltnavn/*Field name***
Sted/*Location*	**Sted/*Location***
Kartblad/*Map*	**Felt, blokknr./*Field, Block No.***
UTM-koordinater/*UTM-coordinates* **Zone: East: North:**	**Koordinater/*Coordinates*** **Projection, datum: East: North:**

Dokumentkontroll/*Document control*

Kvalitetssikring i henhold til/*Quality assurance according to NS-EN ISO9001*

Rev/ *Rev.*	**Revisjonsgrunnlag/*Reason for revision***	**Egenkontroll av/ *Self review by:***	**Sidemanns-kontroll av/ *Colleague review by:***	**Uavhengig kontroll av/ *Independent review by*:**	**Tverrfaglig kontroll av/ *Interdisciplinary review by:***
0	Original document	2016-06-02 KHA	2016-06-02 FLo		

Dokument godkjent for utsendelse/ *Document approved for release*	**Dato/*Date***	**Prosjektleder/*Project Manager***
	2 June 2016	Amir M. Kaynia

NGI (Norwegian Geotechnical Institute) is a leading international centre for research and consulting within the geosciences. NGI develops optimum solutions for society and offers expertise on the behaviour of soil, rock and snow and their interaction with the natural and built environment.

NGI works within the following sectors: Offshore energy – Building, Construction and Transportation – Natural Hazards – Environmental Engineering.

NGI is a private foundation with office and laboratories in Oslo, a branch office in Trondheim and daughter companies in Houston, Texas, USA and in Perth, Western Australia

www.ngi.no

NGI (Norges Geotekniske Institutt) er et internasjonalt ledende senter for forskning og rådgivning innen ingeniørrelaterte geofag. Vi tilbyr ekspertise om jord, berg og snø og deres påvirkning på miljøet, konstruksjoner og anlegg, og hvordan jord og berg kan benyttes som byggegrunn og byggemateriale.

Vi arbeider i følgende markeder: Offshore energi – Bygg, anlegg og samferdsel – Naturfare – Miljøteknologi.

NGI er en privat næringsdrivende stiftelse med kontor og laboratorier i Oslo, avdelingskontor i Trondheim og datterselskaper i Houston, Texas, USA og i Perth, Western Australia.

www.ngi.no

OSLO
TRONDHEIM
HOUSTON
PERTH

NORWEGIAN GEOTECHNICAL INSTITUTE
NGI.NO

Main office
PO Box 3930 Ullevaal St.
NO-0806 Oslo
Norway

Trondheim office
PO Box 5687 Sluppen
NO-7485 Trondheim
Norway

T (+47)22 02 30 00
F (+47)22 23 04 48
NGI@ngi.no

BIC NO. DNBANOKK
IBAN NO26 5096 0501 281
COMPANY NO
958 254 318MVA

ISO 9001/14001
CERTIFIED BY BSI
FS 32989/EMS 612006